BOREAS An international journal of Quaternary research

Sub-arctic Holocene climatic and oceanographic variability in Stjernsund, northern Norway: evidence from benthic foraminifera and stable isotopes

NINA JOSEPH, MATTHIAS LÓPEZ CORREA, JOACHIM SCHÖNFELD, ANDRES RÜGGEBERG AND ANDRÉ FREIWALD

BOREAS

Joseph, N., López Correa, M., Schönfeld, J., Rüggeberg, A. & Freiwald, A. 2013 (July): Sub-arctic Holocene climatic and oceanographic variability in Stjernsund, northern Norway: evidence from benthic foraminifera and stable isotopes. *Boreas*,Vol. 42, pp. 511–531. 10.1111/j.1502-3885.2012.00303.x. ISSN 0300-9483.

A high-resolution record, covering 9.3–0.2 ka BP, from the sub-arctic Stjernsund (70°N) was studied for benthic foraminiferal faunas and stable isotopes, revealing three informally named main phases during the Holocene. The Early- to Mid-Holocene (9.3–5.0 ka BP) was characterized by the strong influence of the North Atlantic Current (NAC), which prevented the reflection of the Holocene Climatic Optimum (HCO) in the bottom-water temperature. During the Mid-Holocene Transition (5.0–2.5 ka BP), a turnover of benthic foraminiferal faunas occurred, Atlantic Water species decreased while Arctic-Polar species increased, and the oxygen isotope record showed larger fluctuations. Those variations correspond to a period of global climate change, to spatially more heterogeneous benthic foraminiferal faunas in the Nordic Seas region, and to regionally diverging terrestrial temperatures. The Cool Late Holocene (2.5–0.2 ka BP) was characterized by increased abundances of Arctic-Polar species and a steady cooling trend reflected in the oxygen isotopes. In this period, our record differs considerably from those on the SW Barents Sea shelf and locations farther south. Therefore, we argue that regional atmospheric cooling triggered the late Holocene cooling trend. Several cold episodes centred at ~8.3, ~7.8, ~6.5, ~4.9, ~3.9 and ~3.3 ka BP were identified from the benthic foraminiferal faunas and the $\delta^{18}O$ record, which correlated with marine and atmospherically driven proxy records. This suggests that short-term cold events may result from reduced heat advection via the NAC or from colder air temperatures.

Nina Joseph (nina.joseph@gzn.uni-erlangen.de), Universität Erlangen-Nürnberg, GeoZentrum Nordbayern, Loewenichstrasse 28, D-91054 Erlangen and Senckenberg am Meer, Abteilung Meeresgeologie, Südstrand 40, D-26382 Wilhelmshaven, Germany; Matthias López Correa (matthias.lopez@gzn.uni-erlangen.de), Universität Erlangen-Nürnberg, GeoZentrum Nordbayern, Loewenichstrasse 28, D-91054 Erlangen, Germany; Joachim Schönfeld (schoenfeld@geomar.de), GEOMAR, Helmholtz-Zentrum für Ozeanforschung Kiel, Wischhofstrasse 1-3, D-24148 Kiel, Germany; Andres Rüggeberg (andres.ruggeberg@ugent.be), Renard Centre of Marine Geology (RCMG), Department of Geology and Soil Science, Ghent University, Krijgslaan 281 S8, B-9000 Gent, Belgium and GEOMAR, Helmholtz-Zentrum für Ozeanforschung Kiel, Wischhofstrasse 1-3, D-24148 Kiel, Germany; André Freiwald (andre.freiwald@senckenberg.de), Senckenberg am Meer, Abteilung Meeresforschung, Südstrand 40, D-26382 Wilhelmshaven, Germany and MARUM, Center for Marine Environmental Sciences, Loebener Strasse, D-28359 Bremen, Germany; *received 20th September 2011, accepted 5th September 2012.*

In recent years, several reconstructions of Holocene palaeoceanographic changes and climate variability have been performed based on planktonic and benthic foraminifera from the shelf areas of the Nordic Seas (Klitgaard-Kristensen *et al.* 2001; Jennings *et al.* 2002; Rasmussen *et al.* 2007) and the Barents Sea (Hald *et al.* 1989; Polyak & Mikhailov 1996; Duplessy *et al.* 2001; Chistyakova *et al.* 2010; Risebrobakken *et al.* 2010), and in fjords along the Norwegian coast (Sejrup *et al.* 2001; Husum & Hald 2004b; Kjennbakken *et al.* 2011). These studies showed that the climate in NW Europe is driven by the interplay between atmospheric and oceanographic control mechanisms such as solar influence and heat transport via the North Atlantic Current (NAC). The poleward heat flux, the position of the oceanic fronts, and the regional climate changed considerably owing to NAC variability (Koç *et al.* 1993, 1996; Hald & Aspeli 1997; Hald *et al.* 2007).

Moreover, Holocene climate records reconstructed from marine and terrestrial archives indicated that the Holocene climate in the Nordic Seas and Barents Sea was not as stable as previously thought (e.g. Bond *et al.* 1997; Mayewski *et al.* 2004; Andersen *et al.* 2004a, b; Nesje *et al.* 2005; Hald *et al.* 2007; Wanner *et al.* 2011). In particular, the relatively warm conditions in the early and middle Holocene were punctuated by several, abrupt cooling phases, centred at 10.0, 9.7, 8.2, 7.9, 6.5, 4.7 and 4.3 cal. ka BP (Andersen *et al.* 2004a, b; Nesje *et al.* 2005; Hald *et al.* 2007; Wanner *et al.* 2011).

Benthic foraminiferal faunas and stable isotope records have proven to be useful tools for reconstructing bottom-water-mass properties, including temperatures (e.g. Sejrup *et al.* 2001; Husum & Hald 2004b; Kjennbakken *et al.* 2011). Seawater oxygen isotope composition and temperature exert the primary control on the oxygen isotope signal incorporated in the calcite tests of foraminifera (McCrea 1950; Emiliani 1955; Shackleton & Opdyke 1973). Benthic foraminifera are restricted in their distribution by a number of environmental parameters, such

DOI 10.1111/j.1502-3885.2012.00303.x

as temperature, salinity, bottom-water oxygenation and trophic regimes (Murray 2006). This becomes evident through a clear zonation of benthic faunal provinces along the shelf in the Nordic Sea region, which can be subdivided into Lusitanian, Boreal, Arctic and Polar (high Arctic) communities (e.g. Feyling-Hanssen 1972; Sejrup *et al*. 1981, 2004; Hald & Steinsund 1992; Corner *et al*. 1996; Hald & Korsun 1997; Husum & Hald 2004a). This zonation can essentially be attributed to the progressive cooling of the northward-flowing Atlantic Water (AW), and to food availability (e.g. Murray 2006). Faunal assemblages of benthic foraminifera can thus be used as proxies for assessing bottom-water changes in shelf areas (e.g. Klitgaard-Kristensen *et al*. 2001; Rasmussen *et al*. 2007; Chistyakova *et al*. 2010) and in fjord settings, which have a deep-water connection to the open shelf (e.g. Sejrup *et al*. 2001; Husum & Hald 2004b).

Here we investigate a gravity core from the moraine-silled Stjernsund trough in northern Norway (70°N). Stjernsund is located at the boreal–arctic boundary in northern Fennoscandia and mimics fully marine conditions resulting from a deep-water connection to the open shelf. Owing to its location and the inflow of the NAC, the benthic ecosystem is supposed to react sensitively to climatic and oceanographic changes, which may originate from southern (boreal) or northern (arctic) regions. It was shown in recent studies that temperature anomalies may be advected into the northern Norwegian region, but may also be caused by local variations in heat flux processes (Furevik 2001; Eilertsen & Skarðhamar 2006). Thus, in addition to heat exchange with the inflowing AW via the NAC, the bottom water in Stjernsund may be affected by heat transfer from the surface and subsurface layers, which are modulated by local meteorology and river discharge (Rüggeberg *et al*. 2011). In Norwegian fjords, the surface-temperature signals typically affect the deepest bottom waters with a delay of about four months with muted amplitude (Eilertsen & Skarðhamar 2006). It was shown that Norwegian fjords have the potential to record atmospheric temperature changes in their bottom waters (e.g. Husum & Hald 2004b). In addition, fjords often act as natural sedimentary traps, and thus allow for Holocene high-resolution studies (e.g. Mikalsen *et al*. 2001; Hald *et al*. 2003).

The aim of this study is to reconstruct fluctuations in the current systems and the local palaeoclimate of the Holocene. The geographic position may enable us to show the importance of local heat flux processes (Furevik 2001; Eilertsen & Skarðhamar 2006) and it may support the south-to-north link between Holocene climate records from the North Sea to the Barents Sea (e.g. Husum & Hald 2004b; Risebrobakken *et al*. 2010). In order to explore the interplay of atmospheric and oceanographic control mechanisms in Stjernsund we (i) reconstruct bottom-water temperatures of the Stjernsund fjord basin based on oxygen isotopes ($\delta^{18}O$); (ii) trace temperature changes and potential variations of the NAC across the Holocene by means of benthic foraminiferal assemblages; and (iii) compare our proxy records with other regional marine and terrestrial climate proxy records.

Regional setting and oceanography

The Stjernsund (Fig. 1) at 70°N in Norway is an east–west-trending glacial trough connected to the open shelf of the Barents Sea in the west and to the Altafjord at its eastern end (e.g. Freiwald *et al*. 1997). The Stjernsund trough is up to 3.5 km wide and ~30 km long. The Alta River, which flows into the Altafjord, accounts for the low-saline surface water layer, while the bottom water is constituted by inflowing NAC water (Rüggeberg *et al*. 2011). A Lateglacial terminal moraine forms a distinct sill within the trough (López Correa *et al*. 2012) about half-way between Altafjord and the Barents Sea embayment near Lopphavet. The examined gravity core lies within the SE part of the trough that was occupied by an ice stream during the Younger Dryas (López Correa *et al*. 2012), and the trough sediments are thus exclusively postglacial. This terminal moraine sill acts today as a barrier for the inflowing AW, and divides the Stjernsund into an outer (NW) and inner (SE) trough, of 410 and 480 m water depth. The sill crest depth varies between 236 and 203 m, and its flanks are covered by the prominent cold-water corals *Lophelia pertusa* and *Madrepora oculata* (Freiwald *et al*. 1997; Rüggeberg *et al*. 2011; López Correa *et al*. 2012), reflecting the permanent influence of AW.

The main water-masses found on the shelf off the northern Norwegian coast and in the studied fjord are of Atlantic and coastal origin (Hopkins 1991; Skarðhamar & Svendsen 2005; Rüggeberg *et al*. 2011). The Norwegian Atlantic Current (NwAC) represents the main part of the relatively warm (>8°C) and saline (>35) NAC, which continues along the Norwegian continental slope into the Barents Sea as a bottom-water-mass in the North Cape Current (NCaC), and towards the north (West Spitsbergen Current – WSC; Fig. 1). Near the coast, the NAC is capped by low-saline surface water of the Norwegian Coastal Current (NCC; Dullo *et al*. 2008). The NCC originates primarily from the freshwater outflow of the Kattegat and the Baltic Sea and from Norwegian mainland runoff (Mork 1981; Fig. 1). The NCC flows northwards, parallel to the coast, and stretches out as a thin wedge beyond the shelf edge. NCC waters are comparatively low-saline (<35) and extend down to >50–250 m (Hopkins 1991; Skarðhamar & Svendsen 2005; Rüggeberg *et al*. 2011). Norwegian Sea Deep Water (NSDW), with salinities of

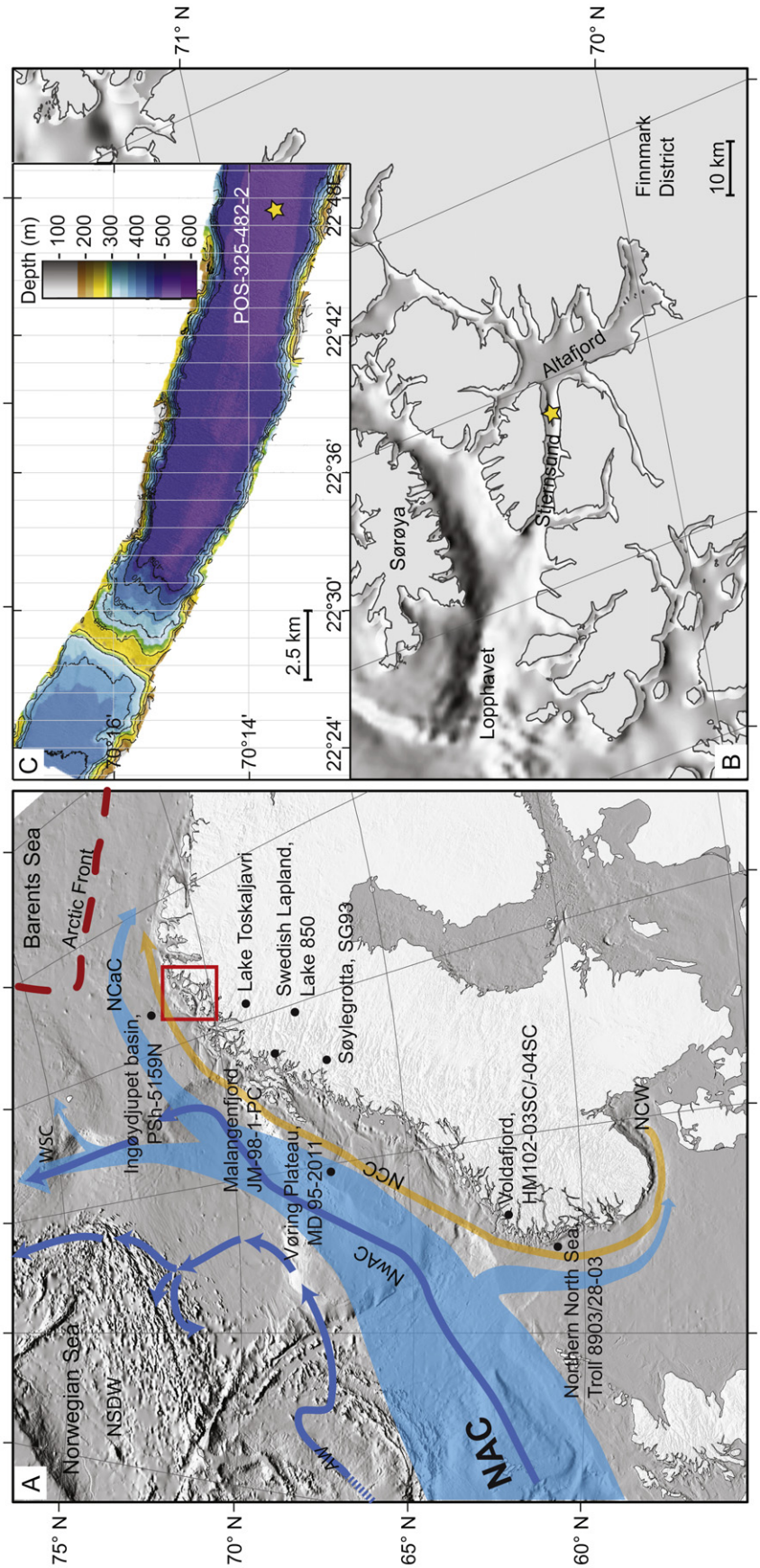

Fig. 1. A. Nordic Seas index map with the main currents, water-masses and frontal systems (after Drange *et al.* 2005; Dullo *et al.* 2008; Azimuthal-projection, GEBCO-bathymetry). Surface currents: NAC = North Atlantic Current; NCaC = North Cape Current; NCC = Norwegian Coastal Current; NwAC = Norwegian Atlantic Current; WSC = West Spitzbergen Current. Water-masses: AW = Atlantic Water; NSDW = Norwegian Sea Deep Water; NCW = Norwegian Coastal Water. Oceanic fronts: AF = Artic Front. B. Regional map of the Stjernsund (rectangle in A), with location of the investigated gravity core POS-325-482-2 marked by an asterisk. C. Multibeam bathymetry of the Stjernsund (modified after López Correa *et al.* 2012), showing the 497-m-deep glacial trough and the Younger Dryas terminal moraine sill at ~250 m water depth.

<34.95 and temperatures of <0°C, prevails below ~800 m along the continental margin west of the study area (Skarðhamar & Svendsen 2005).

In Stjernsund, the AW is the dominant water-mass below ~150 m (Rüggeberg *et al*. 2011). Different water-mass distributions east and west of the sill were indicated by hydrographical investigations. CTD cast time series showed the permanent AW presence west of the sill, while AW flushes over the sill into the SE trough twice a day during high tide and partly mixes with lower-salinity fjord waters (Rüggeberg *et al*. 2011). Despite the sill, the tidally driven AW inflow faithfully refills the SE trough with AW, and the conditions in this inner basin at the coring site POS-325-482-2 are fully marine. Based on the slight salinity difference, the residual AW component within this basin is >99.3% (López Correa *et al*. 2012). The Stjernsund sedimentary record is thus suitable for reconstructing climate variations in connection with fluctuations of the NAC. Owing to its location inshore from the transition of the Norwegian Sea into the Barents Sea, the benthic fauna is oceanographically governed by the inflowing warm AW, but may be further climatically influenced by cold air masses from the Arctic realm through atmospheric cooling of the fjord water body. The postglacial sediments recovered in the Stjernsund fjord basin are hence well suited to record the interplay between marine and atmospheric influences.

Materials and methods

Core description

This study is based on the 566-cm-long gravity core POS-325-482-2 (Figs 1, 2), collected from 479 m water depth (70°13′85″N, 22°47′63″E) in the eastern fjord basin during RV 'Poseidon' cruise POS-325 in July and August 2005 (Freiwald *et al*. 2005). The sediments are homogenous silty clays, which scarcely show bioturbation structures. In some sections of the core, isolated vertical polychaete burrows of ~5 cm in length were found. They showed a black lining, while other bioturbation features appeared to be minimal. A few scaphopods (*Siphonodentalium lobatum*) and small double-valved bivalves (*Pseudamussium sulcatum*, *Bathyarca frielei*, *Delectopecten vitreus*, *Nucula* sp.) were found sporadically, as well as a large gastropod (*Neptunea* sp.) and a solitary coral, *Flabellum macandrewium*. Fine-grained homogenous silty clays constitute the lower part of the core (566 to 120 cm), and few fine-sand-enriched horizons were present. The upper core part (120 to 0 cm) comprises coarse silty clay with a higher proportion of fine sand.

Chronology

The chronostratigraphy of core POS-325-482-2 has been established with seven radiocarbon ages (Fig. 2;

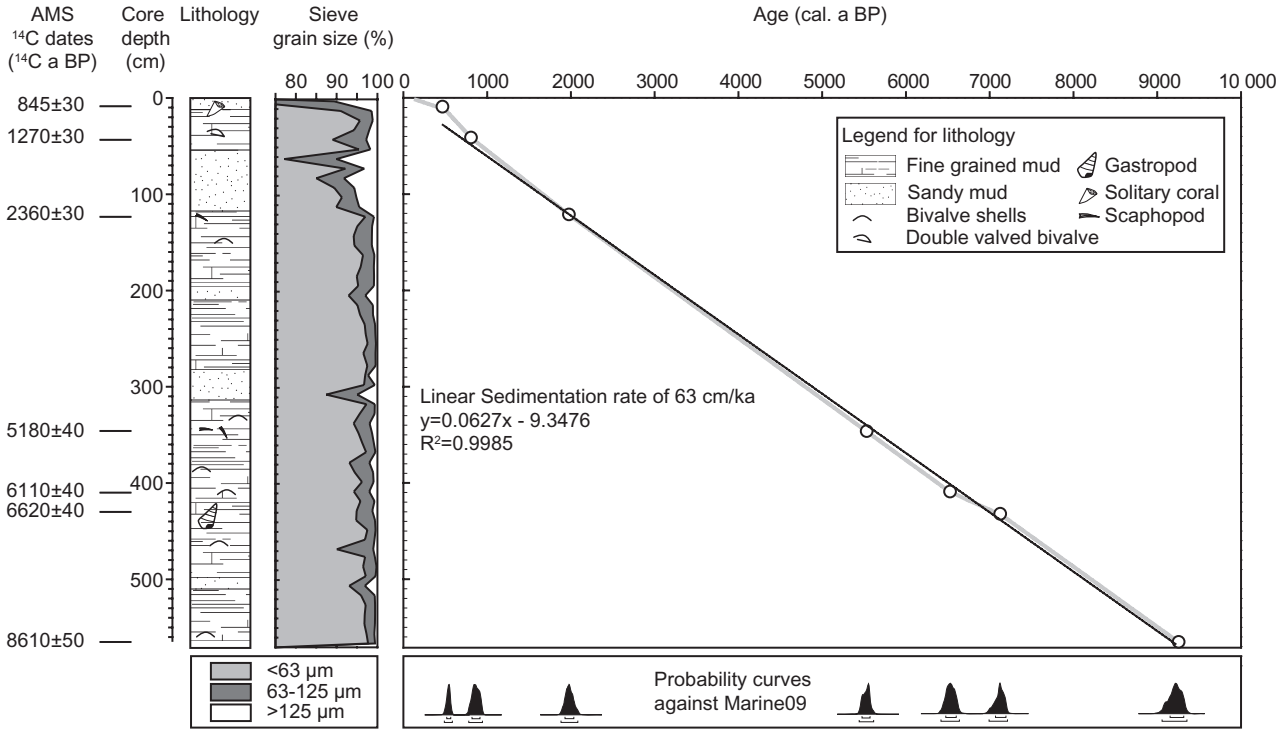

Fig. 2. The lithology with the position of AMS ^{14}C dates indicated, the sieve grain-size distribution versus core depth (cm), and the age model of core POS-325-482-2, including the probability curves with ranges of 2σ.

Table 1. Radiocarbon dating results (AMS-^{14}C) of core POS-325-482-2 and calibrated age ranges. The calibration was done in OxCal 3.10, using the Marine09 calibration (Reimer *et al.* 2009). Calibrated age ranges (not corrected for local ΔR) represent the 2σ confidence interval of the respective probability curves. Data marked with an asterisk are from López Correa *et al.* (2012).

Sample	Depth (cm)	Species	^{14}C-Lab. code	AMS-^{14}C (^{14}C a BP)	Calibrated age range (cal. a BP)
STJ-482-10*	10	*Flabellum macandrewium*	Poz-24325	845±30	525–425
STJ-482-42	42	*Pseudamussium sulcatum*	Poz-42317	1270±30	900–730
STJ-482-122	122	*Siphonodentalium lobatum*	Poz-42314	2360±30	2090–1880
STJ-482-347	347	*Siphonodentalium lobatum*	Poz-42315	5180±40	5630–5450
STJ-482-410	410	Bivalve fragments	Poz-42316	6110±40	6650–6420
STJ-482-433*	433	*Neptunea* sp.	Poz-24324	6620±40	7250–7020
STJ-482-566	566	*Bathyarca frielei*	Poz-42318	8610±50	9420–9110

Table 1) of calcareous hard parts of well-preserved benthic fauna, namely the solitary coral *Flabellum macandrewium* (10 cm), the gastropod *Neptunea* sp. (433 cm), scaphopods (122 and 347 cm) and bivalve shells (42, 410 and 566 cm). Radiocarbon dating was performed at the Poznań Radiocarbon Laboratory with an Accelerator Mass Spectrometer (AMS). The resulting ages are reported in Table 1 as radiocarbon years (^{14}C a BP) and as calibrated age ranges (cal. a BP). AMS-^{14}C ages were calibrated with the program OxCal 3.10 against the marine calibration data set Marine 09 (Reimer *et al.* 2009) to derive calibrated ages. Calibrated age ranges in Table 1 correspond to the 2σ ranges of the resulting probability curves (Fig. 2). In the following, all ages are given in calibrated years BP, that is, years (a) or thousand years (ka) before AD 1950.

Sampling and sample preparation

The core was sampled every 10 cm for benthic foraminifer stable isotope analyses, and for benthic foraminiferal assemblages. The samples comprise a section interval of 2 cm. The wet weight of the sediment was measured, and the sample then dried at 60°C in a ventilated drying cabinet. The weight reduction was controlled every 12 h until a consistent dry weight plateau was reached, which was the case after 72 h for all samples. Subsequently, the dried sediment samples were soaked overnight in dilute hydrogen peroxide (10%) to facilitate a sufficient disintegration and separation of adherent fine-grained sediment from foraminiferal shells (Wick 1947). The low H_2O_2 concentration and short soaking time ensured that arenaceous foraminifera were not destroyed, if they had been preserved at all in the reducing conditions of potentially anoxic pore waters of the sediment core. The suspended sample was then washed through nested sieves of 63-, 125- and 250-μm mesh size. Sediment grains >250 μm were not present in this core. Each fraction was collected from the sieves with distilled water to prevent particle clumping during drying and stored in pre-weighted 100-mL Nunc cups. The fractions of 63–125 μm and >125 μm were dried at 45 to 50°C for 24 h and then weighed, which allowed for a rough constraint on grain size distribution, which was expressed as weight percent.

Benthic foraminifera

The analyses of the benthic foraminiferal assemblages were carried out on the >125-μm size fraction, which is widely used for benthic foraminiferal studies because it allows the most secure identification of foraminiferal species. Smaller, juvenile specimens in the 63–125 μm fraction may lack the diagnostic morphological features of adult individuals, and examination of the 125-μm fraction facilitates microscopic work on samples rich in fine detrital sand (Hermelin 1986). Not only juveniles but also small and environmentally sensitive forms, for instance some *Bolivina, Epistominella* and *Stainforthia* species, were lost when a size fraction larger than 63 μm was examined (Schröder *et al.* 1987). Literature data inferred that 49% of the living specimens and 28% of the species inventory were not captured in the >125-μm fraction as compared to the >63-μm fraction (Schönfeld 2012). However, in the present case of fjord basin core POS-325-482-2, different *Stainforthia* species as well as a rich fauna of bolivinids were recorded (Tables S1, S2 in Supporting Information). *Epistominella exigua* was also present, which usually has a size distribution maximum around 125 μm (Gooday 1993). As such, the loss of environmental information from studying the >125-μm fraction is considered minimal in the present study.

The samples were split with an Otto-microsplitter to obtain an aliquot containing at least 300 specimens. The whole aliquot was picked and counted. Species were identified to species/genus level and kept separately in KRANTZ micro-cells. The foraminiferal census data were transferred into relative species abundance data and referred to the dry sample weight to obtain benthic foraminiferal numbers (BFN) per gram

sediment as absolute abundances. The number of planktonic foraminifera was registered in connection with the benthic quantitative analysis, but these foraminifera were not analysed in detail for this study. Fisher's α diversity was calculated with the program PAST 2.01 (Hammer & Harper 2008).

To identify structures in the data sets of the relative abundance of benthic foraminifera, multivariate analyses were performed with PAST 2.01 (Hammer & Harper 2008). In order to reduce species numbers to a practical level, only those species that occurred in at least one sample among the five most abundant species were taken into account, which resulted in a reduction to 20 species. In addition, *Pullenia* spp. (*Pullenia bulloides* and *P. quinqueloba*) were included in the analyses because of their association with Atlantic-derived water (Lohmann 1978; Belanger & Streeter 1980; Risebrobakken *et al*. 2010).

Stable isotopes

For stable isotope measurements, the benthic foraminiferal species *Cassidulina laevigata* and *Cassidulina neoteretis* were picked from the fraction >125 to <250 μm. Visually clean specimens of similar test size (125 to 250 μm) without signs of dissolution were chosen. Generally, 10–20 specimens of *C. laevigata* and 15–20 specimens of *C. neoteretis* were used for each measurement to achieve the required sample weight of at least 0.04 mg $CaCO_3$. The foraminifera were coarsely crushed, and cleaned with methanol in an ultrasonic bath. The measurements were carried out with a ThermoFinnigan MAT 252 mass spectrometer at the GeoZentrum Nordbayern at the University of Erlangen. Based on replicate measurements of an internal carbonate standard, the reproducibility for $\delta^{18}O$ and $\delta^{13}C$ is ±0.03‰, respectively. The stable isotope values are given in the delta-notation relative to the Vienna Pee Dee Belemnite (V-PDB) carbonate standard. Between 568 and 214 cm core depth, *C. neoteretis* was measured. Because this species was scarce in the upper 214 cm of the core, *C. laevigata* was measured instead. Between 214 and 2 cm, eight parallel measurements of both species were carried out to determine if the resulting stable isotope values show a systematic species-dependent offset. A tentative bottom-water temperature was calculated on the basis of the benthic $\delta^{18}O$ record using the equation of Shackleton (1974):

$$T\,(°C) = 16.9 - 4.0(\delta^{18}O_{foraminifer} - \delta^{18}O_{water}). \quad (1)$$

The modern seawater oxygen isotope composition $\delta^{18}O_{water}$ is 0.22±0.06‰ VSMOW, and the stable carbon isotope composition of dissolved inorganic carbon (DIC) in seawater is $\delta^{13}C_{DIC}$=0.50±0.04‰ VPDB (S. Flögel, pers. comm. 2012).

Results

Age model and sedimentation rate

Radiocarbon dating yielded ages between 845±30 ^{14}Ca BP at 10 cm and 8610±50 ^{14}C a BP at 566 cm, which correspond to calibrated ages between 475 and 9265 cal. a BP. The calibrated ages, listed in Table 1, form a near-linear age vs. depth relationship, which corresponds to an overall sedimentation rate of ~63 cm ka^{-1} from ~9.3 to ~0.5 ka BP (Fig. 2). The 10-cm spacing of the 57 samples, analysed for foraminiferal assemblages and stable isotopes, corresponds to an average resolution of 165 years, while each 2-cm-wide sampling interval thus represents ~33 years on average. The sedimentary record shows a maximum bioturbation and hence vertical homogenization depth of ~5 cm. The 10-cm sample spacing thus ensures a sufficient signal separation.

Sieve grain-size distribution

The grain-size distribution revealed that the >125-μm fraction contributes with 0.2–2.0% and the >63-μm fraction with 0.7–5.0% to the sediment record in the lower 454 cm (Fig. 2). Increased proportions of coarse grained material (>125 μm) were recorded at 506, 468, 307, 287 and 204 cm core depth. In the upper 112 cm, the >125-μm fraction contributes 1–10%, with highest proportions at 82, 62 and 2 cm core depth. The >63-μm fraction contributes with 2–22%, and highest proportions are displayed again at 82, 62, 42 and 2 cm core depth (Fig. 2). Coarse non-biogenic grains (>125 μm) in the record were composed of mica, mafic minerals and in some samples quartz.

Stable isotopes

The benthic $\delta^{18}O$ values vary between 3.0 and 3.3‰ V-PDB from the beginning of the record at ~9.3 until ~5.0 ka BP, except for excursions towards heavier values at ~8.3, ~7.8 and ~6.5 ka BP (Fig. 3A). Further excursions towards heavier values occur at ~4.9, ~3.9 and ~3.3 ka BP. The $\delta^{18}O$ excursions at ~8.3, ~7.8, ~6.5 and ~4.9 ka BP have a magnitude of ~0.5 to ~0.7‰ relative to immediately adjacent values, and cover time-spans of 200 to 400 years. The $\delta^{18}O$ excursions at ~4.9 and ~3.3 ka BP display $\delta^{18}O$ values that are even 1‰ heavier than the values in horizons directly above and below. The $\delta^{18}O$ variability is generally higher between ~5.0 and ~2.5 ka BP, and ranges from 2.2 to 4.3‰. The lightest $\delta^{18}O$ value is recorded at ~2.8 ka BP, with 2.2‰. After ~2.5 ka BP the $\delta^{18}O$ values increase steadily from 2.6 to 4.0‰ at ~0.5 ka BP. This trend is only interrupted by a short decrease between ~1.6 and ~1.2 ka BP. For the period between ~3.5 and ~0.2 ka BP, the $\delta^{18}O$ of the eight sample pairs of *C. laevigata* and *C. neoteretis* from the same horizon reveal differences varying between 0.1 and 0.5‰ (average $\delta^{18}O$ offset 0.15‰).

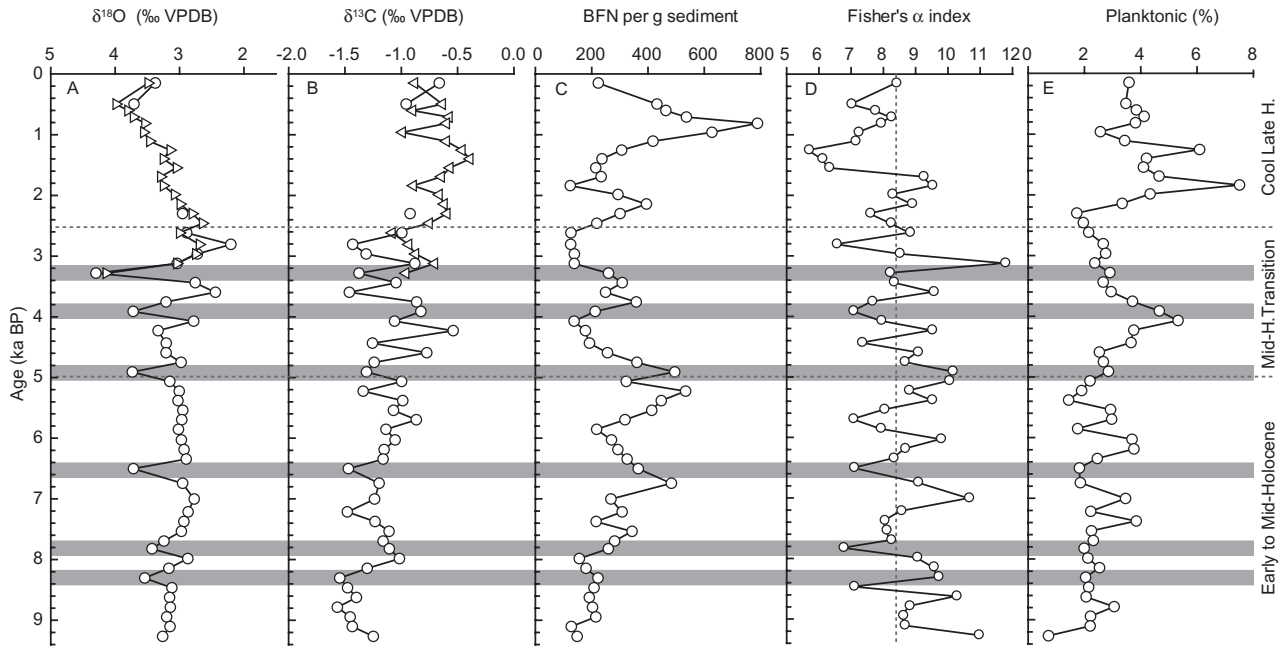

Fig. 3. The benthic $\delta^{18}O$ (A) and $\delta^{13}C$ (B) records of *Cassidulina laevigata* (triangles) and *Cassidulina neoteretis* (circles); benthic foraminiferal numbers (BFN) per gram sediment (C); Fisher's α diversity index (D); and the proportion of planktonic foraminifera (E). Dashed horizontal lines indicate the subdivision of the Holocene into three intervals, and grey-shaded bars mark cold episodes.

The $\delta^{13}C$ values vary between –0.4 and –1.5‰ (Fig. 3B), with a generally increasing trend between ~9.3 and ~0.2 ka BP. Slightly higher $\delta^{13}C$ start at ~2.5 ka BP, coincident with the onset of the steady $\delta^{18}O$ increase across the late Holocene (Fig. 3A). Paired measurements of *C. laevigata* and *C. neoteretis* revealed no systematic offset between the two species, with $\delta^{13}C$ differences ranging between 0.09 and 0.5‰ (0.19‰ on average).

Benthic foraminifera

A total of 92 benthic foraminiferal species belonging to 53 genera were identified in core POS-325-482-2 (Table S1). There were fewer than 50 planktonic foraminifera in each sample, and their proportion was <8% of the entire foraminiferal fauna (Fig. 3E). The benthic foraminifera were well preserved and showed no signs of dissolution. The benthic foraminiferal number (BFN) ranges from 123 to 789 specimens per gram dry sediment. Between ~9.3 and ~5.0 ka BP, the BFN values increased from ~120 to ~450 specimens per gram dry sediment. Generally lower BFN values (120 to 360 ind. g^{-1}) were recorded between ~5.0 and ~2.5 ka BP. Increased values were displayed from ~2.5 to ~0.4 ka BP, with BFN values ranging between ~300 and ~800 specimens per gram dry sediment. The uppermost sample at 2 cm (~0.2 ka BP) shows only ~120 specimens per gram dry sediment (Fig. 3C).

Fisher's α index ranged from ~5.5 to ~12.0 with an average of 8.4, implying higher diversity at higher values (Fig. 3D). It displays low-amplitude variations around the average value between ~9.3 and ~2.6 ka BP. Between ~2.6 and ~1.7 ka BP values were between 7.5 and 9.0. Values below the average were displayed between ~1.7 and ~0.5 ka BP, with only the surface sample (~0.2 ka BP) displaying a value that is at the average (Fig. 3D). Minimum values of 7 or lower were recorded at ~8.4, ~7.8, ~6.5, ~5.7, ~4.5, ~3.9, ~3.3 and ~2.8 ka BP. Most minima in the Fisher's α correspond to excursions of the $\delta^{18}O$ record towards heavier values (Fig. 3A), except at ~5.7, ~4.5 and ~2.8 ka BP.

Species grouping and abundance. – Correspondence analysis was applied to the reduced data set of the 20 most frequent benthic foraminiferal species including *Pullenia* spp. to obtain species associations with distinct distributions or preferences for certain environmental conditions. From the 57 samples, correspondence analysis extracted 18 axes. The two first axes were clearly separated from the others by their percentage of total variance, and they accounted for 72% of the total data variability (Fig. 4). Species scores fall into three main groups that are referred to as Assemblage 1 to 3. There was also one outlier (*Brizalina skagerrakensis*), which is considered separately.

Assemblage 1 was characterized by high positive Axis 2 and high negative Axis 1 scores. It is composed of *Melonis barleeanum*, *C. neoteretis* and *Cibicidoides pachyderma*, species that are known as AW indicators (Atlantic Water group; e.g. Lubinski *et al.* 2001; Rytter

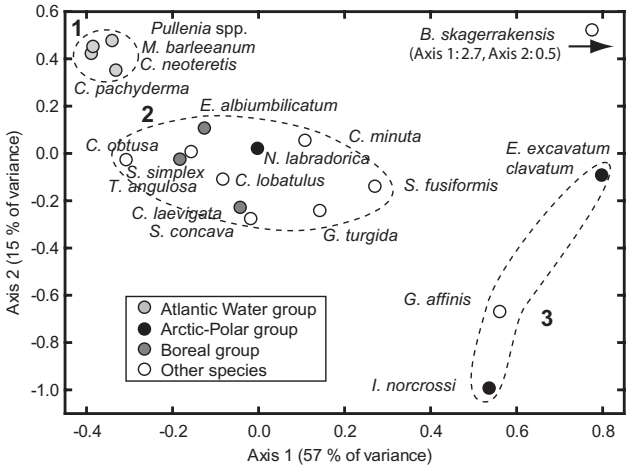

Fig. 4. Correspondence analysis of the relative abundances of the 20 species that occurred among the five most abundant in at least one sample and *Pullenia* spp. from core POS-325-482-2. Assemblage 1 represents the Atlantic Water group, assemblage 2 includes among others the Boreal group, and assemblage 3 includes Arctic-Polar species.

et al. 2002; Rasmussen *et al*. 2007). Assemblage 2 was determined by positive and negative Axis 1 and 2 scores. This assemblage was predominantly composed of boreal species, in particular *Elphidium albiumbilicatum*, *Cassidulina obtusa*, *Trifarina angulosa*, *Cassidulina minuta*, *C. laevigata*, *Stainforthia concava*, *Globobulimina turgida*, *Stainforthia fusiformis*, *Nonionellina labradorica*, *Spirorbina simplex* and *Cibicides lobatulus*. Assemblage 3 was characterized by high positive Axis 1 and negative Axis 2 values. This assemblage is represented by the two Arctic-Polar species *Elphidium excavatum clavatum* and *Islandiella norcrossi*, joined by *Globobulimina affinis. Brizalina skagerrakensis* yielded an outstanding positive Axis 1 score (2.7) and also a comparatively high positive Axis 2 score (0.5). This species has very different dynamics from the others because it occurs only in the uppermost part of the core and it is considered as an outlier.

The obtained assemblages correspond approximately to recent benthic faunal provinces (Lusitanian, Boreal, Arctic-Polar) that were identified along the shelf in the Nordic Seas region (e.g. Feyling-Hanssen 1972; Sejrup *et al*. 1981, 2004; Hald & Steinsund 1992; Corner *et al*. 1996; Hald & Korsun 1997; Husum & Hald 2004a). Thus we grouped the benthic foraminiferal species of Stjernsund into an Arctic-Polar group represented by *E. excavatum clavatum*, *I. norcrossi* and *N. labradorica*, and a Boreal group formed by *T. angulosa*, *C. laevigata*, *E. albiumbilicatum* and *Hyalinea balthica*. The Boreal group commonly includes species that are indicative for Atlantic-derived waters, such as *C. neoteretis*, *M. barleeanum* and *Pullenia* spp. (e.g. Lubinski *et al*. 2001; Rytter *et al*. 2002; Rasmussen *et al*. 2007). Because these species formed a separate assemblage in the correspondence analysis they are treated here as a separate group (Fig 4). The relative abundances of the most important species are given in Fig. 5.

The Boreal group accounts for 34% on average of the benthic fauna. Its proportions are below average between 566 and 486 cm and between 62 and 2 cm core depth. Between 476 and 184 cm, values show an overall increasing trend and they are above the average between 214 and 72 cm core depth (Fig. 5). *Cassidulina laevigata* is, with proportions between 13 and 48.5%, the main contributor to this group. Associated species are *E. albiumbilicatum* and *T. angulosa* with proportions between 1 and 6%. *Hyalinea balthica* appears at 6.7 ka BP, and the proportions vary between 0 and 3% (Fig. 5).

The Atlantic Water group accounts for 20% on average of the benthic fauna. Between 566 and 224 cm, values are close to or above the average. The proportion of the Atlantic Water group decreases below average at 214 cm and shows a rather abrupt drop at 134 cm to less than 7%. Its proportions remains that low until 2 cm core depth (Fig. 5). *Cassidulina neoteretis* is most abundant between ~9.3 and 2.3 ka BP, with proportions of 7.5–28%, while its proportions are much lower, 0.5–4%, from ~2.3 to 0.2 ka BP (Fig. 5). *Melonis barleeanum* and *C. pachyderma* show distribution patterns similar to *C. neoteretis*. Both species are frequent between ~9.3 and 3.5 ka BP, with proportions ranging from 1.5 to 9.5%, but both decrease rapidly at ~3.5 ka BP to proportions between 0 and 3.5% (Fig. 5). *Pullenia bulloides* and *P. quinqueloba* together show maximum abundances of 1.4–3.6% between ~9.3 and 8.0 ka BP, and decrease steadily towards the core top (Fig. 5).

The Arctic-Polar group occurs on average with 14%. Values above the average are displayed from 536 to 526 cm, from 486 to 448 cm, from 418 to 378, at 204 cm and from 132 to 2 cm core depth (Fig. 5). *Nonionellina labradorica* is one of the most common species; it occurs with proportions between 4 and 22%. *Elphidium excavatum clavatum* and *Islandiella norcrossi* are rare before ~2.5 ka BP (Fig. 5). Their abundance increases from ~2.5 to ~0.2 ka BP.

Discussion

Age model and sedimentation rates

The age model revealed a constant sedimentation rate of 63 cm ka^{-1} between ~9.3 and ~0.4 ka BP (Fig. 2). Based on this rate, the surface age (at 2 cm) was extrapolated and yielded 149 cal. a BP. The core covers most of the Holocene sedimentation after the retreat of the Younger Dryas ice stream from the SE trough. The virtually constant sedimentation rate throughout the last ~9.3 ka justifies the linear age model that was applied to the palaeoceanographic data sets. The

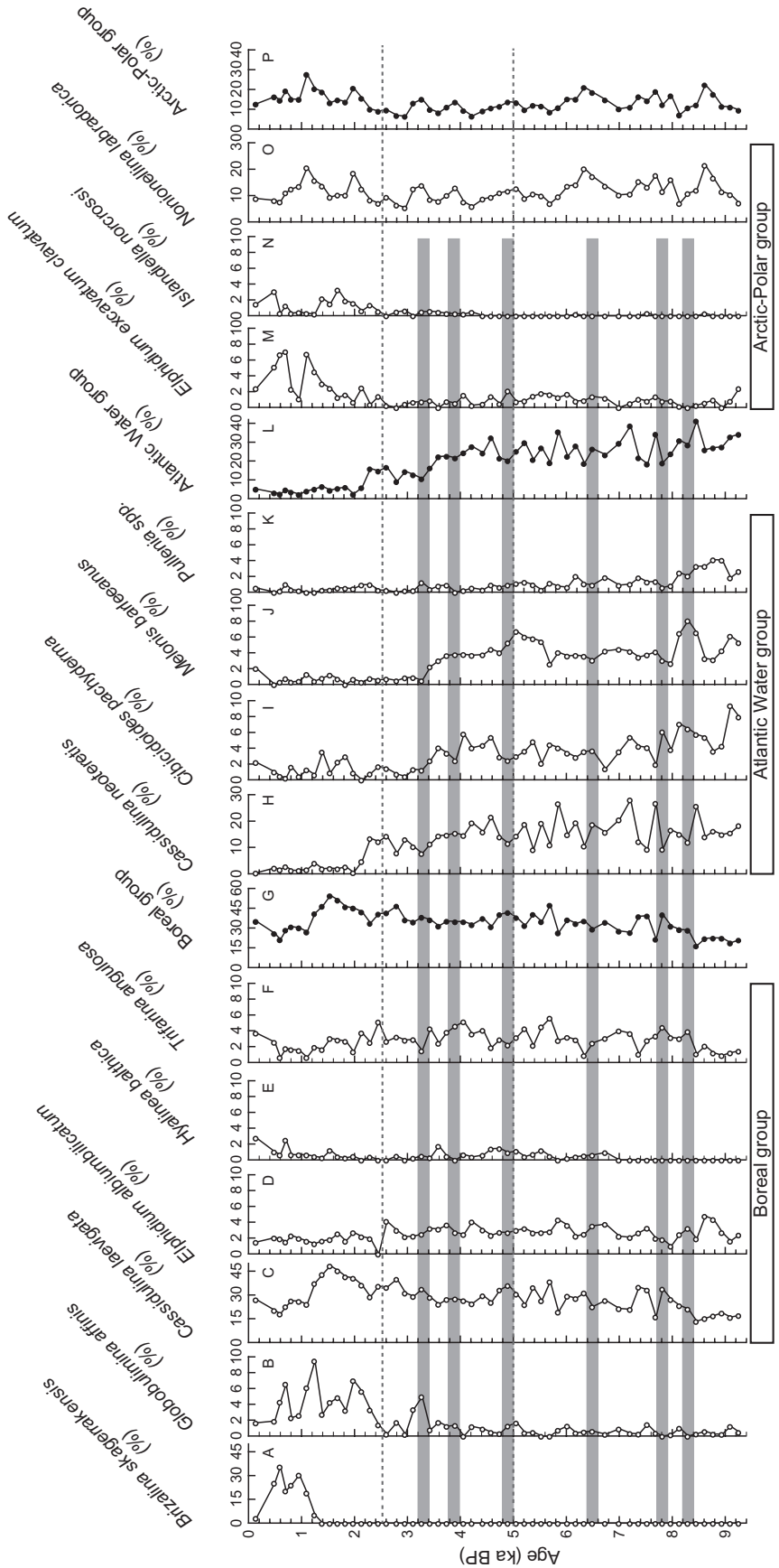

Fig. 5. The percentages of the most common benthic foraminiferal species, the Boreal (C-G), the Atlantic Water (H-L), and the Arctic-Polar (M-P) groups. Grey bars indicate cold events and dashed lines the subdivision of the Holocene into three intervals. Note that the *x*-axes have different scales to allow for better visibility of abundance trends.

calibrated ages (Table 1, Fig. 2) have not been corrected for local reservoir effects (ΔR), as the full history of ΔR at the site throughout the Holocene is not completely known. The only periods with available local ΔR from Stjernsund (López Correa *et al.* 2012) show mean values (±stdv.) of 99±54 years (4 measurements) between 9.8 and 9.4 ka BP and of 20±21 years (4 measurements) between 3.2 and 1.8 ka BP. While the correction for the youngest core part would be minimal, we would see improved fits of the observed cold events in Stjernsund to other climate and ocean records (discussed below) if a ~99-year age correction were applied to the early Holocene core part between ~9.3 and ~7.6 ka BP.

The sedimentation rate of ~63 cm ka^{-1} in Stjernsund is higher by a factor of ~8 than on the adjacent SW Barents Sea shelf, as revealed from core PSh-5159N from Ingøydjupet (Risebrobakken *et al.* 2010). The strong contrast between the in-shore sedimentation and the open-shelf deposition reflects the protected situation behind the terminal moraine sill. The majority of the suspended sediment load is deposited in the fjord basin and leaves the open shelf relatively starved. The large sedimentation rate renders the Stjernsund fjord basin an ideal site for high-resolution time series. The rapid deposition rate is comparable to that in similar moraine-silled fjords, such as the Malangenfjord (Troms District), which yielded an overall sedimentation rate of 75 cm ka^{-1} across the last 9 ka in core MD99-2298 (Hald *et al.* 2003). Lower rates of 29 cm ka^{-1} have been documented in the Voldafjord in the More and Romsdal District (Kjennbakken *et al.* 2011), but likewise with a nearly constant rate across several millennia.

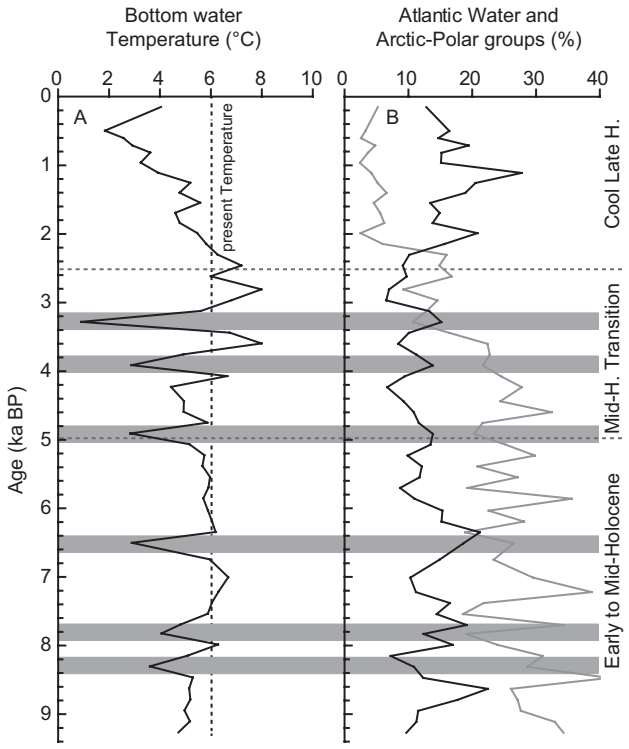

Fig. 6. A. Reconstructed temperatures calculated from the benthic foraminifer $\delta^{18}O$ record. B. The relative abundances of the Atlantic Water group (grey line) and the Arctic-Polar group (black line) in core POS-325-482-2.

Palaeo-environment in Stjernsund

The benthic foraminiferal distribution and the stable isotope record of the core allowed a subdivision of the Holocene into three intervals (Figs 3, 5, 6). They are informally named Early to Mid-Holocene (~9.3 to ~5.0 ka BP), Mid-Holocene Transition (~5.0 to ~2.5 ka BP) and Cool Late Holocene (~2.5 to 0.2 ka BP). This subdivision is based on changes that were observed in several parameters of core POS-325-482-2 and should not be considered as a standard subdivision of the Holocene. In general, trends and changes in the stable isotope record coincide with changes in the distribution of benthic foraminiferal groups (Fig. 6). The Early to Mid-Holocene from 9.3 to 3.5 ka BP is characterized by the Atlantic Water group, indicating a strong influence of the NAC. The stable isotope record suggests comparatively warm and stable conditions, except for short excursions that point to periodic cold spells. The Mid-Holocene Transition is characterized by a faunal turnover and increased variation of the stable isotope record, which suggest that temperature and food supply probably changed as a result of a more restricted NAC influence in the fjord basin. It is suggested that the influence of atmospheric temperatures increased during the mid- to late Holocene. The Cool Late Holocene is marked by an increase of the Arctic-Polar group and continuously increasing $\delta^{18}O$ values, which both indicate a continued cooling. The strong cooling of the bottom water is interpreted to relate primarily to a generally colder climate, probably in combination with decreased NAC export strength.

Reconstructed bottom-water temperatures and stable isotopes. – Compared with later periods, the stable oxygen isotope record suggests constant and warm temperatures in the Early to Mid-Holocene, with the exception of several excursions towards heavier values. Higher amplitudes of $\delta^{18}O$ values during the Mid-Holocene Transition suggest increased temperature variability. Continuously colder conditions are indicated in the Cool Late Holocene by increasing $\delta^{18}O$ values. In general, episodes of heavier $\delta^{18}O$ values are accompanied by increased abundance of Arctic-Polar species, which supports temperature as the primary control of the benthic oxygen isotope record in Stjernsund. It is assumed that the $\delta^{18}O$ record in core POS-325-482-2 was not influenced by glacial meltwater, as the glacial coverage in Finnmark was similar to or even

less than today's after ~9.3 ka BP (Corner *et al.* 1990; Rea & Evans 2007). López Correa *et al.* (2012) showed with coupled ^{14}C and Neodymium isotope signatures in U-series-dated cold-water corals on the terminal moraine sill that a strong influence of meltwater occurred only until ~9.5 ka BP in Stjernsund. Moreover, the Stjernsund $\delta^{18}O$ record shares the same overall $\delta^{18}O$ window as the adjacent open-shelf record from Ingøydjupet (Risebrobakken *et al.* 2010). However, reduced meltwater influx during cold periods may potentially enrich local seawater $\delta^{18}O$ to more NAC-like compositions, owing to increased salinity, and thus apparently colder conditions. The youngest (~0.2 ka BP) reconstructed bottom-water temperature is 4°C. CTD-casts in August 2005 east of the sill revealed bottom-water temperatures of 6°C (Rüggeberg *et al.* 2011). The offset of ~2°C may be explained by the overall temperature rise in the last ~150 years (e.g. Hass 1996; Overland *et al.* 2004; Eiríksson *et al.* 2006; Bjune *et al.* 2009; Seppä *et al.* 2009), which is not captured with the uppermost sample of core POS-325-482-2.

In Stjernsund, $\delta^{18}O$ differences between the species *C. neoteretis* and *C. laevigata* vary between 0.1 and 0.5‰ and do not support a consistent offset (Fig. 3A). The offset may be attributed to different microhabitat depth within the sediment, as well as to calcification during different parts of a season. However, we see no systematic offset between the $\delta^{18}O$ values of the two species. This is in contrast to the earlier statement by Poole (1994), who showed a systematic offset.

It has been stated in previous studies that *C. neoteretis* calcifies its shell in near equilibrium (-0.02 ± 0.22‰) with the ambient water in terms of oxygen isotope composition, while *C. laevigata* shows 0.19 ± 0.13‰ lower $\delta^{18}O$ values (Poole 1994). A species-specific vital effect has been questioned for instance by Kjennbakken *et al.* (2011), who concluded that systematically larger amplitudes in *C. laevigata* than in *Uvigerina mediterranea* could be the result of test production during one season or one part of a season. It has been observed that *C. laevigata* produces its test during short periods of phytodetritus deposition (Gooday & Lambshead 1989) and thus reflects only one season or one part of a season, as suggested by Kjennbakken *et al.* (2011), namely probably early spring. Other studies suggested that varying $\delta^{18}O$ differences between species might be related to environmental effects, such as seasonality (Austin & Scourse 1997), or to post-mortem calcite dissolution (Schmiedl & Mackensen 2006). A dissolution effect would cause simultaneously increased $\delta^{18}O$ and $\delta^{13}C$ values (Wu & Berger 1989), but the records do not show a consistent signature supporting this, which suggests that the variable differences between the species are not primarily caused by dissolution.

In Stjernsund, the lowest $\delta^{13}C$ values were recorded in the early Holocene between 9.3 and 8.2 ka BP (Fig. 3B), indicating a high organic matter flux to the fjord basin. Slightly higher fluctuations are displayed between 5.0 and 2.5 ka BP, which infer changing food supply conditions, during the Mid-Holocene Transition. In the Cool Late Holocene $\delta^{13}C$ values are highest, suggesting reduced organic matter flux to the fjord basin. More negative $\delta^{13}C$ values during the early- and mid-Holocene in Stjernsund may result from a higher organic matter flux owing to higher primary productivity in the surface water, because phytodetritus discriminates towards ^{12}C (Filipsson & Nordberg 2010).

Benthic foraminiferal groups. – In general, trends and changes in the bottom-water temperatures coincide with changes in the proportion of benthic foraminiferal groups (Fig. 6).

The Atlantic Water group is associated with (chilled) Atlantic water-masses of the NAC that carry heat and particulate organic matter into northern regions (Mackensen *et al.* 1985; Mackensen & Hald 1988; Hald & Steinsund 1992; Rasmussen *et al.* 2007). Species of this group are present throughout the Holocene, which reflects the continuous influence of AW in Stjernsund bottom waters (Fig. 5). Their relative abundance decreased continuously during the Holocene, while the proportion of Arctic-Polar species that are adapted to colder bottom water increased (Fig. 5). In this study, the Atlantic Water group is interpreted to reflect general changes in temperature and food supply, which are related to the export strength and the local influence of the NAC, rather than to water-mass changes. Individual species showed different timings of decreasing abundances (Fig. 5), which may relate to their different optimum conditions regarding temperature and food supply (Mackensen & Hald 1988; Caralp 1989; Mackensen *et al.* 1993; Heinz *et al.* 2001; Rytter *et al.* 2002).

The Boreal group shows a comparatively constant pattern throughout the Holocene, except for lower abundances in the early and late Holocene (Fig. 5). Species of this group are rather opportunistic and tolerate, for instance, salinity changes (Mackensen & Hald 1988; Corner *et al.* 1996; Klitgaard-Kristensen *et al.* 2002).

The Arctic-Polar group is frequently found in highly productive areas close to frontal zones between Arctic and Polar Waters and/or near the sea-ice edge (Hald & Steinsund 1992). The species *N. labradorica* has a wide temperature range (Conradsen 1995), but its maximum abundance (>20%) is in colder waters where temperatures are lower than ~2°C (Sejrup *et al.* 2004). *E. excavatum clavatum* and *I. norcrossi* are characteristic of Arctic-Polar conditions and are abundant in glaciomarine fjords (Hald & Aspeli 1997; Korsun & Hald 1998; Sejrup *et al.* 2004) and in the Baltic Sea today, where *E. excavatum clavatum* prefers the deeper areas within and below the halocline (Lutze 1965, 1974; Nikulina *et al.* 2008). Increased abundances of the Arctic-Polar group in Stjernsund are interpreted to reflect colder

conditions in the bottom water. This is supported by a close relationship between the relative abundance of the Arctic-Polar group and the $\delta^{18}O$ temperature reconstruction.

Early to Mid-Holocene (~9.3 to ~5.0 ka BP). – During the Early to Mid-Holocene, bottom-water temperatures are between 4 and 7°C, except for cool episodes at ~8.3, ~7.9 and ~6.5 ka BP, when temperatures of <4°C are suggested by the $\delta^{18}O$ signal (Fig. 6A). They are interpreted as cold episodes, which is further supported by increased proportions of the Arctic-Polar group, and will be discussed separately. The benthic foraminiferal fauna is characterized by the Atlantic Water group with proportions >20% (Fig. 6B), suggesting a strong influence of the NAC in the fjord basin. In modern fjords, *C. neoteretis*, *Pullenia* spp. and *M. barleeanum* are found in Atlantic water-masses with temperatures between 6 and 7.9°C and at salinities between 34.0 and 35.1 (Husum & Hald 2004a). Another common species in this interval is *C. laevigata*. Its abundance increased in the early Holocene at ~8.2 ka BP and remained fairly constant in the middle Holocene. The immigration of this species into Norwegian fjord settings after the Younger Dryas is indicative of the successive warming of bottom water to 6–8°C (Sejrup *et al.* 2001). The estimated temperature of ~6°C for this interval is at the lower limit of the temperature indicated by the foraminiferal assemblage but appears plausible. The abundance of mainly Boreal and Atlantic Water species and the scarcity of species with Arctic-Polar affinity (Figs 5, 6B) argue for strong Atlantic Water influence and warm bottom-water temperatures in the fjord basin. Low $\delta^{13}C$ values suggest high organic matter flux to the sea floor (Rohling & Cooke 1999; Maslin & Swann 2006; Schulz & Zabel 2006). This is supported by high abundances of species preferring high organic matter supply (Figs 3, 5) such as *M. barleeanum*, *N. labradorica* and *P. bulloides* (Caralp 1989; Mackensen *et al.* 1993; Rytter *et al.* 2002). Planktonic foraminifera were scarce in the fjord trough deposits, at <4%. The scarcity could be explained by the prevalence of low-salinity surface and subsurface waters in Stjernsund (Rüggeberg *et al.* 2011) and by the intolerance of planktonic species to low-salinity waters (Kucera 2007). However, their abundance increased slightly throughout the early and middle Holocene (Fig. 3E). For the Early to Mid-Holocene period it can be assumed that the environment was characterized by stable Atlantic Water conditions and high organic matter flux.

Mid-Holocene Transition (~5.0 to ~2.5 ka BP). – In the period between ~5.0 and ~2.5 ka BP, temperatures fluctuate between 1 and 8°C, and show minimum values at ~4.9, ~3.9 and ~3.3 ka BP (Fig. 6B). The abundance of the Atlantic Water group significantly decreases across the Mid-Holocene Transition (Fig. 6B), which suggests that the influence of the NAC changed and resulted in different temperature and food conditions. Increased fluctuations of the $\delta^{18}O$ and $\delta^{13}C$ signals suggest enhanced temperature and food supply variability, which may be related to higher seasonal variability (see discussion on *C. laevigata* above). Species such as *C. laevigata* and *E. albiumbilicatum* still show high abundances (Fig. 5), which can be explained by their ability to successfully withstand changing conditions (Schmiedl 1995; Corner *et al.* 1996; Nikulina *et al.* 2008). The turnover in the benthic foraminiferal fauna is probably also influenced by eustatic uplift and a relative sea-level fall of ~10 m, which constricted the space over the sill for the inflowing NAC between 9.4 and 3.2 ka BP (López Correa *et al.* 2012). These latter authors assumed that the NAC inflow might have played a stronger role during the early Holocene, while the influence of the tidal currents probably increased as a consequence of the constricted space. Thus today's regime was imposed with AW sweeping over the sill only twice a day (Rüggeberg *et al.* 2011), while the remaining AW component in the fjord basin bottom water is ~99.6% (López Correa *et al.* 2012). The more restricted inflow of AW and the lowered sea level probably rendered the water-masses of the fjord basin SE of the sill more susceptible to atmospheric influences. It was shown that bottom-water temperatures in shallower fjord basins, such as Malangen (~250 m), correlate with the decreasing insolation at high northern latitudes following the orbital forcing and with atmospheric signals. This implies a close coupling between ocean and atmosphere regarding heat transfer processes (Husum & Hald 2004b).

Cool Late Holocene (~2.5 to ~0.2 ka BP). – During the late Holocene temperatures drop continuously from approximately 8°C at ~3.0 ka BP to 2°C at ~0.4 ka BP (Fig. 6A). At ~0.2 ka BP, temperatures increase again to 4°C, while recent temperatures are ~5.9°C (Rüggeberg *et al.* 2011). Fisher's α index of benthic foraminiferal diversity drops below 8.5 at 1.5 ka BP (Fig. 3D), suggesting less favourable conditions (Gooday 1993; Murray 2006). The increased abundance of the Arctic-Polar group (Fig. 6B) supports cooler bottom-water temperatures than in the previous intervals. Cooling of the fjord bottom water is also mirrored in the significantly decreased diversity (Sejrup *et al.* 2001) and low abundance of species with warm AW affinity (Figs 3D, 5, 6B). The latter phenomenon reflects the generally decreased influence of the NAC in Stjernsund compared with the Early to Mid-Holocene. The colder climate in the region (Shemesh *et al.* 2001; Seppä & Birks 2002; Risebrobakken *et al.* 2010) and decreased export strength of the NAC since ~4.0 ka BP (Ślubowska-Woldengen *et al.* 2008) probably enhanced cooling of the bottom water.

For the late Holocene, heavier $\delta^{13}C$ values suggest lower primary production. By contrast, the benthic foraminiferal record indicates increased organic matter supply by the abundance of the deep infaunal species *G. affinis* (Corliss & Emerson 1990; Schönfeld 2001; Fig. 6). The species does not occur in the North Atlantic at pelagic flux rates lower than ~3.5 g C m^{-2} a^{-1} and tolerates dysoxic conditions (Corliss & Emerson 1990; Schönfeld 2001; Geslin *et al.* 2004). Phytodetritus transported from the surface ocean has been shown to be its preferred food source (Nomaki *et al.* 2006). The increased burial of organic carbon would preferentially remove ^{12}C from seawater, so that the ocean reservoir would become isotopically heavier (Bickert 2006). Higher transport of organic matter into the sediment and the increased abundance of *G. affinis* point to periodically decreased ventilation.

Correlation with other ocean and land proxy records

The water-masses in Stjernsund are closely connected to the water-masses of the NAC and the Norwegian Coastal Current containing Norwegian Coastal Water (NCW) that has its origin in the Baltic Sea (NCC; Fig. 1). Therefore climatic processes taking place farther south can influence northern coastal water, as can interactions between the NCC and the AW in the NAC (Eilertsen & Skarðhamar 2006). It was assumed that temperature anomalies can be advected into the northern Norwegian region, but can also be caused by local variations in heat flux processes (Furevik 2001; Eilertsen & Skarðhamar 2006). Thus, in addition to changing heat and volume transports of the AW flow through the Nordic Seas (Furevik 2001), the bottom water in Stjernsund may be affected by heat transfer from the surface and subsurface layers, which are modulated by local meteorology and river discharge (Rüggeberg *et al.* 2011). Today, the surface temperature signals reach the deepest bottom waters with a delay of about four month in Norwegian fjords (Eilertsen & Skarðhamar 2006). Depending on the depth of the fjord and connectivity to the open shelf this signal is muted to varying degrees, but fjord bottom waters are clearly affected by the local atmospheric temperature regime (e.g. Husum & Hald 2004b). In addition, the inflow and strength of AW in the North Atlantic is also linked to atmospheric circulation (Hurrell *et al.* 2003). Depending on the atmospheric forcing, the heat transport through the NAC will increase or decrease (Blindheim *et al.* 2000). Atmospheric temperature changes are roughly reflected in sea-surface temperature (SST) variability (Furevik 2001), in reconstructions from pollen records (e.g. Bjune *et al.* 2004; Seppä *et al.* 2009) and in speleothems (Lauritzen & Lundberg 1999).

In order to elucidate fluctuations in the current systems as well as to investigate the influence of seaborne heat transfer mechanisms (Furevik 2001) and local heat flux related to local climate changes (Eilertsen & Skarðhamar 2006) during the Holocene, the Stjernsund record is compared with other marine and terrestrial records with independent age models (Figs 7, 8) along a south–north profile from the northern North Sea to the SW Barents Sea (Fig. 1).

The marine records reflect variations in the current systems. Changes in the inflow of AW to the Norwegian Channel are reflected in the frequency of the benthic foraminifer *Uvigerina mediterranea* (Klitgaard-Kristensen *et al.* 2001). Along the Norwegian shelf, the AW inflow is recorded in the concentration of the coccolithophorid *Gephryocapsa muellerae* (Vøring Plateau; Giraudeau *et al.* 2010) and in the benthic foraminiferal stable isotope record from the SW Barents Sea (Risebrobakken *et al.* 2010). SST from the summer mixed layer based on alkenones reflects the influence of atmospheric temperatures resulting from summer insolation at high northern latitudes (Calvo *et al.* 2002; Risebrobakken *et al.* 2010). The benthic foraminiferal stable isotope record of Malangenfjord showed that bottom-water temperatures are correlated with atmospheric temperatures as well as with fluctuations of AW flow along the path of the NAC (Husum & Hald 2004b). Owing to the analogous setting, it is assumed that the bottom-water temperatures in Stjernsund were driven by similar processes. The terrestrial records are surface ground temperatures inferred from speleothem data (Lauritzen & Lundberg 1999), July mean temperatures on the basis of pollen (Seppä & Birks 2002), and $\delta^{18}O$ values from lacustrine diatoms (Shemesh *et al.* 2001), which are supposed to reflect atmospheric temperatures (climate).

Long-term climatic variation. – The overall decreasing trend of species associated with AW conditions in Stjernsund corresponds well with the decreasing abundance of *Uvigerina mediterranea* recorded in the northern North Sea (Klitgaard-Kristensen *et al.* 2001; Fig. 7F). Investigations in this region and in the west Norwegian Voldafjord showed that the benthic foraminifer *U. mediterranea* is closely connected with AW and reflects changes in the inflow of AW into the Norwegian Channel (Klitgaard-Kristensen *et al.* 2001; Sejrup *et al.* 2001). In addition, these records are in step with the general temperature decrease observed in Malangenfjord, western Norway, as well as in SST records from Ingøydjupet Basin (PSh-5159N, SW Barents Sea) and Vøring Plateau (MD952011). These records follow the generally decreasing summer insolation at 65°N (Figs 6B, 7C, D, 8E). They also follow the decreasing temperature inferred from $\delta^{18}O$-based records in Greenland (Johnsen *et al.* 2001; Vinther *et al.* 2009). The overall similarity of these records implies a close coupling in the ocean–atmosphere climatic system.

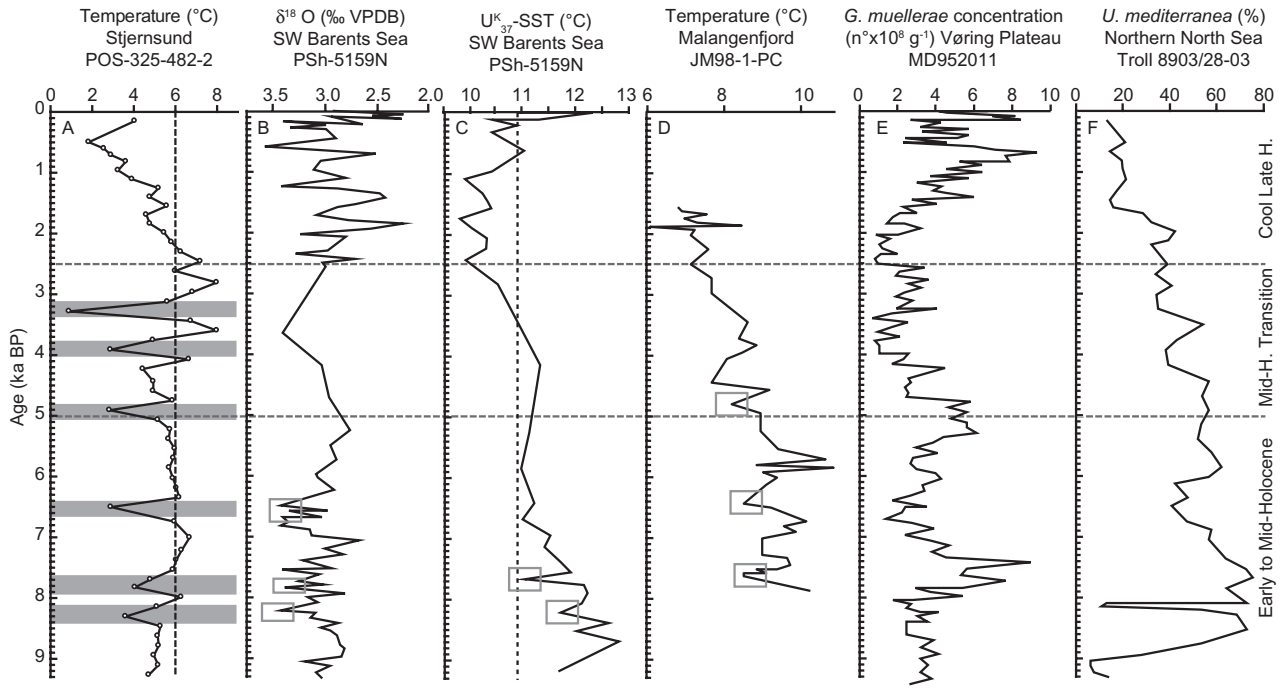

Fig. 7. The reconstructed bottom-water temperature, 479 m water depth, for the Stjernsund (A) compared with marine proxy records along a north–south transect. The benthic $\delta^{18}O$ record of *Cassidulina neoteretis* (B) and summer sea-surface temperature (SST) reconstruction based on alkenones (C), from the SW Barents Sea (Ingøydjupet basin), 422 m water depth (Risebrobakken *et al*. 2010). Temperature reconstruction for the Malangenfjord based on $\delta^{18}O$ values from benthic foraminifera (Husum & Hald 2004b; D). The site-specific coccolith concentration in core MD952011 from the Vøring Plateau (Giraudeau et al. 2010; E). The relative abundance of *Uvigerina mediterranea* from Troll 8903/28-03, northern North Sea (Klitgaard-Kristensen *et al*. 2001; F). Grey shaded areas indicate cooling events observed in Stjernsund, grey squares in other proxy records indicate possible correlations, and dashed lines indicate the subdivision of the Holocene.

The Holocene Climatic Optimum (HCO) is a prominent feature in many early to middle Holocene records (e.g. Calvo *et al*. 2002; Kaufman *et al*. 2004; Jansen *et al*. 2008; Renssen *et al*. 2009; Andersson *et al*. 2010). By contrast, the bottom-water temperature trend in Stjernsund is characterized by stable conditions with average temperatures similar to those of today. Similarly, the benthic foraminifer $\delta^{18}O$ record of core PSh-5159N (Fig. 7B) and the speleothem record SG93 (Fig. 8D) from northern Norway do not display a pronounced HCO. Warmer temperatures were recorded in alkenone-based SST reconstructions from the mid-Norwegian margin (Fig. 8E) and from the adjacent SW Barents Sea shelf (Fig. 7C), as well as in the bottom-water temperature record of Malangenfjord (Fig. 7D). Considerable discrepancies in SST reconstructions have been observed between phytoplankton and zooplankton proxies from North Atlantic records (Jansen *et al*. 2008; Andersson *et al*. 2010; Risebrobakken *et al*. 2011). The absence of the HCO in the benthic record of Stjernsund and the adjacent shelf supports the argument of Jansen *et al*. (2008) that the lack of HCO in the temperature reconstructions based on foraminifera and radiolarians rules out increased advection of warmer AW (Koç *et al*. 1993; Kaufman *et al*. 2004) as an explanation for the HCO. Instead, it was proposed that the HCO is solely the response to the radiative forcing owing to the orbital configuration at the time (Jansen *et al*. 2008). This hypothesis is supported by modelling results, which show that the different proxies respond to different mechanisms (Risebrobakken *et al*. 2011). Proxies from the summer mixed layer reflect decreasing summer insolation at high northern latitudes, while proxies below this layer are assumed to reflect the mean state of the NAC. The discrepancy between Malangenfjord and Stjernsund, which are both strongly influenced by AW, may be explained by the shallower water depth in Malangenfjord (~250 m). There, bottom-water temperatures are more closely related to atmospheric forcing factors (Husum & Hald 2004a, b) than in the deeper Stjernsund (~480 m), especially in the early Holocene. Overall, comparison with other proxy records emphasized that the benthic record of the Stjernsund was driven by constant heat transport through the NAC, which provided stable bottom-water temperatures despite the higher temperatures at the sea surface, except for short cold episodes (see discussion below).

During the Mid-Holocene Transition (5.2–2.5 ka BP), a gradually decreasing abundance of the Atlantic Water group and increased temperature fluctuations (4–7°C) in the Stjernsund bottom water are displayed.

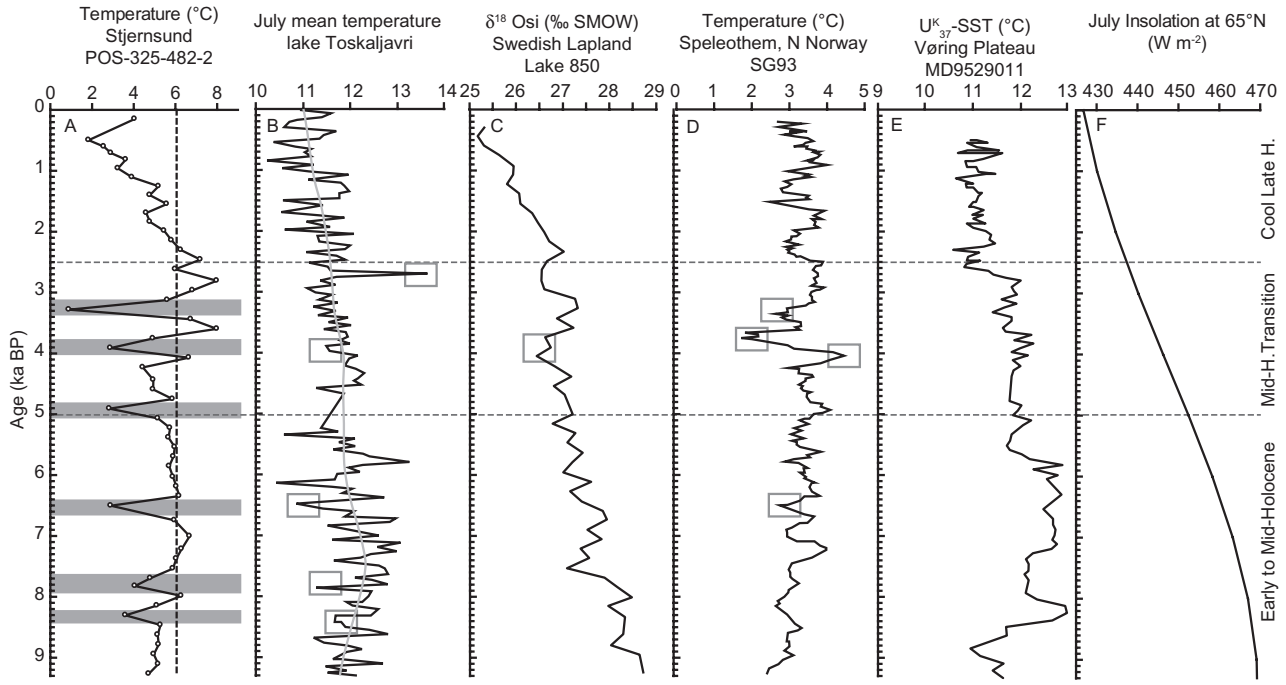

Fig. 8. The reconstructed bottom-water temperature, 479 m water depth, for the Stjernsund (A) compared with atmospherically driven proxy records along a north–south transect. Atmospheric July mean interpreted on the basis of pollen (Seppä & Birks 2002; B). Lacustrine $\delta^{18}O_{si}$ values (Shemesh *et al.* 2001; C). Temperature reconstruction based on the speleothem record in Søylegrotta, Arctic Circle (66°N) (Lauritzen & Lundberg 1999; D). Summer sea-surface temperature (SST) reconstruction based on alkenones, Vøring Plateau, 1048 m water depth (Calvo *et al.* 2002; E). Summer insolation at 65°N (Berger & Loutre 1991; F). Grey shaded areas indicate cooling events observed in Stjernsund, grey squares in other proxy records indicate possible correlations, and dashed lines indicate the subdivision of the Holocene.

SST reconstructions based on alkenones display gradually colder surface waters during summers (Figs 7C, 8E), and the benthic record of Malangenfjord indicates decreasing bottom-water temperatures (Fig. 7D). Pollen-based July mean and annual mean temperatures show a roughly linear cooling trend over the last ~5000 years (Fig. 8B; Seppä & Birks 2002; Bjune *et al.* 2004; Seppä *et al.* 2009). The trends in the latter records correlate well with decreasing insolation at 65°N (Fig. 8F). However, the faunal turnover and the increased temperature fluctuations in the Stjernsund occur during a period of global rapid climate change (Mayewski *et al.* 2004). The higher amplitudes of temperature change in Stjernsund suggest periods with exceptionally high or low temperatures. Pollen records display warm and cold anomalies during the last 5000 years, despite the overall cooling trend (Seppä & Birks 2001, 2002; Bjune *et al.* 2004). The inferred cooling of bottom water at ~3.9 ka BP and the anomalously high temperatures at ~4.1 and ~2.7 ka BP correlate well with lower and higher July mean temperatures in lake Toskaljavri (Seppä & Birks 2002), and with increased temperature changes of >2°C in the speleothem record (Lauritzen & Lundberg 1999), respectively (Fig. 8B, D). This suggests a close coupling between the ocean and the atmosphere in Stjernsund. A gradual lowering of the sea level (~10 m between 6.0 and 2.5 ka BP) in the area (Romundset *et al.* 2011) probably resulted in a more restricted AW exchange compared to the early Holocene (López Correa *et al.* 2012) and may have had the effect that bottom-water temperatures became more susceptible to atmospheric changes compared to the early Holocene. The effect may have been enhanced by a general weakening of the NAC (Ślubowska-Woldengen *et al.* 2008). It has been demonstrated that sea-surface and air temperatures were well intercorrelated in fjords along the mid to northern Norwegian coast and that the atmospheric signal from surface-water layers is transported to bottom-water layers in fjords (Eilertsen & Skarðhamar 2006).

In the Cool Late Holocene period (2.5–0.2 ka BP), the abundance of Arctic-Polar species in Stjernsund increased, while the Atlantic Water group strongly decreased after ~1.8 ka BP (Fig. 6B). This interval was characterized by a continuous decrease in bottom-water temperatures from 7°C at the beginning of the late Holocene to 2°C at ~0.4 ka BP, which suggests decreased heat transfer via the inflowing NAC and/or increased heat loss to the atmosphere. Decreased NAC export strength since ~4.0 ka BP is assumed from several shelf records (Ślubowska-Woldengen *et al.* 2008). This is in line with lower abundances of *U. mediterranea* in the Norwegian Channel (Fig. 7F) and low concentrations of *G. muellerae* at the Vøring Plateau

until ~1 ka BP (Fig. 7E). In the nearby Ingøydjupet basin, proportions of species associated with AW are high (66±8%) after ~2.4 ka BP (Risebrobakken *et al.* 2010). However, the high abundance of AW species on the SW Barents Sea shelf is due to the high abundance of *Alabaminella weddellensis* (reported in Risebrobakken *et al.* 2010 as *Eponides weddellensis*). This species is associated with the deposition of phytodetrital aggregates, which originate in the euphotic zone and settle rapidly to the sea floor following the spring bloom (Gooday 1993). Therefore its high abundance probably results from increased food availability rather than from the influence of warmer AW carried by the NAC. Thus, initial cooling of the bottom water in Stjernsund in the late Holocene may relate to decreased heat advection through the NAC.

The $\delta^{18}O$ values of Stjernsund reflect a change that would correspond to an absolute temperature decrease of ~4°C. By contrast, the $\delta^{18}O$ record of the adjacent shelf (Fig. 7B) does not show any cooling trend. Therefore it is assumed that Stjernsund is additionally influenced by local heat transfer processes (Eilertsen & Skarðhamar 2006). The cooling trend in Stjernsund is in line with an atmospheric cooling in Swedish Lapland of similar magnitude (Fig. 8C), which has been interpreted as an increase in the influence of the Arctic polar continental air mass that carries depleted precipitation (Shemesh *et al.* 2001). The change in $\delta^{18}O_{si}$ was estimated to correspond to a temperature decrease of 2.5–4°C (Shemesh *et al.* 2001). July mean temperatures reconstructed from pollen analysis in lake Toskaljavri (Seppä & Birks 2002) support a cooling of about 1°C over the last 2.5 ka BP (Fig. 8B). Remarkably, the temperature record based on speleothem data from northern Norway (Lauritzen & Lundberg 1999) displays rather constant temperatures throughout the late Holocene (Fig. 8D). This discrepancy could be due to the location of the cave farther south, indicating that potential colder air masses from the Arctic polar realm did not penetrate into this region. A colder climate in the northern Norwegian region is also supported by the marine record of Risebrobakken *et al.* (2010), who found episodes of increased influence of coastal water in the SW Barents Sea, which were interpreted as a northward expansion of the NCC under predominantly cold conditions and reduced southwesterly wind strength (Ingvaldsen 2005). A colder climate would result in less warming of the surface layers and increased heat loss of the bottom water (Furevik 2001). Because the Stjernsund basin is deeper than, for instance, Malangenfjord, the heat induced by the inflowing AW could not countervail against the cooling induced by colder surface waters in the late Holocene.

The reconstructed absolute temperature change of ~4°C in Stjernsund is clearly higher than the ~0.5–1°C decrease across the last 2 ka observed in northern Fennoscandian lakes and other circum-Arctic records (Bjune *et al.* 2009; Kaufman *et al.* 2009; Seppä *et al.* 2009). Thus, it seems conceivable that the severe cooling in Stjernsund resulted from a locally colder climate owing to the increased influence of Arctic polar air masses. Decreased heat export strength of the NAC (Ślubowska-Woldengen *et al.* 2008) and lower summer insolation (Berger 1978; Berger & Loutre 1991) may have additionally supported cooling of the bottom water in Stjernsund. The youngest value for bottom-water temperature showed an increase of 2°C, which may relate to the temperature rise in the last ~150 years (e.g. Hass 1996; Eiríksson *et al.* 2006; Bjune *et al.* 2009; Seppä *et al.* 2009).

Short-term variations (cold events). – The reconstructed temperature record at the Stjernsund study site POS-325-482-2 shows millennial-scale cold events at ~8.3, ~7.8, ~6.5, ~4.9, ~3.9 and ~3.3 ka BP (Fig. 3A). These events (except for the one at ~8.3 ka BP) coincide with increased proportions of the Arctic-Polar group (Fig. 6) and with significantly lower diversities (Fig. 3D). The amplitude of the temperature drop for the two events in the early Holocene (~8.3, ~7.9 ka BP) is 2°C, while it is ~3°C for the three following events (~6.5, ~4.9, ~3.9 ka BP), and for the ~3.3 ka BP event it is >5°C. A high abundance of Arctic-Polar species and low diversity are recorded shortly before the $\delta^{18}O$ excursion at ~8.3 ka BP. Increased grain size and higher quartz grain content in the >125-μm fraction between ~8.5 and ~8.3 ka BP may indicate IRD. This cold event is the only one that seems to correlate with one of the cold events described in the North Atlantic by Bond *et al.* (1997). With a correction for the mean ΔR of 99±54 years for the early Holocene in Stjernsund (López Correa *et al.* 2012) applied to our age model, this cold event would exactly match the so-called '8.2-event' (e.g. Rohling & Pälike 2005). This event coincides with the date of the Storegga tsunami at ~8.2 ka BP (Bondevik *et al.* 2012), which affected also the shores of the southern Barents Sea region (Romundset & Bondevik 2011) and thus may have affected the benthic ecosystem in Stjernsund. Furthermore, our record also correlates with a temperature decrease of ~1°C in the SST record of the adjacent shelf (Risebrobakken *et al.* 2010) and with a higher $\delta^{18}O$ value in the benthic record of *C. neoteretis* (reported as *C. teretis*) at the same site (Fig. 7C, G), which support cooling of surface and bottom waters. Suggested mechanisms and forcing factors behind the suborbital millennial to decennial climate variability, superimposed on the insolation-driven temperature decline, are, for example, a combination of solar radiation variability, periods of increased explosive volcanism, and internal feedback mechanisms of the climate system such as the North Atlantic Oscillation (e.g. Calvo *et al.* 2002;

Hald *et al.* 2007; Wanner *et al.* 2011). Remarkably, almost all cold events in Stjernsund coincide with lower July mean temperatures (Fig. 8A, B) in northern Finland (Seppä & Birks 2002), supporting the localized nature of air–sea thermal balance in northern Norwegian fjords (Eilertsen & Skarðhamar 2006). The speleothem record of Søylegrotta (Lauritzen & Lundberg 1999) shows colder intervals around ~8.2, ~7.0, ~6.5, ~3.7 and ~3.4 ka BP (Fig. 8D). Cooler intervals have also been recorded in Malangenfjord (Hald *et al.* 2003; Husum & Hald 2004b). There, the benthic $\delta^{18}O$ record indicates cooling of 1–2°C around ~7.6, ~6.5, ~4.8, ~4.5 and ~1.9 ka BP (Fig. 7D), which has been interpreted as reduced influence of AW (Husum & Hald 2004b). Coccolithophorid concentrations indicative for the flow of AW (Giraudeau *et al.* 2010) suggest weakening of the NAC before ~7.9, at ~6.8–6.4, and at ~4.0–3.8 ka BP (Fig. 7E). The benthic $\delta^{18}O$ record of the SW Barents Sea supports lower temperatures of the AW at ~7.9–7.5 and ~6.8–6.4 ka BP (Fig. 7B; Risebrobakken *et al.* 2010). However, the pattern of reduced AW flow does not coincide with all cooling events in Stjernsund; for example, at ~8.3 and at ~4.9 ka BP increased flow of AW was indicated (Fig. 7E). With regard to the effect of increased influence of Arctic polar air masses in the late Holocene (Shemesh *et al.* 2001), it can be presumed that at least some cold events were primarily induced by the short-term influence of cold air masses. Changing climate conditions may partly be a result of the nature of the key atmospheric circulation processes in northern Europe (e.g. Seppä *et al.* 2009). At present, there are two typical situations: (i) a predominant zonal circulation with a strong Icelandic low-pressure system associated with moist and mild winters; and (ii) the development of a high-pressure cell over Fennoscandia (Scandinavia, Finland, Kola Peninsula, Karelia) resulting in a blockage of the westerly air stream, leading to a meridional-type circulation (Johanessen 1970; Hurrell *et al.* 2003). The latter situation allows for cold air from Arctic polar regions to penetrate farther south and thus induce increased heat loss from sea to air.

It seems conceivable that the cooling of the bottom water in Stjernsund may result (i) from reduced heat transfer owing to decreased NAC export strength, and, probably more importantly, (ii) from colder air temperatures. This is supported by pollen-based July mean and annual mean temperature reconstructions, which conclude that cold (and warm) anomalies are typical of northern Europe and that their occurrence may be related to the oceanic and atmospheric circulation variability in the North Atlantic–North European region (Seppä *et al.* 2009). Likewise, recent observations have shown that cold and warm anomalies may be induced either by advection of AW or by air temperatures (Furevik 2001).

Conclusions

- The overall decreasing abundance of the Atlantic Water group across the Holocene in Stjernsund is indicative of locally decreasing inflow of AW, which probably resulted from eustatic uplift that constricted the space above the sill for the inflowing NAC. The low abundance in the Cool Late Holocene (2.5–0.2 ka BP) may relate to a general weakening of the NAC.
- Benthic foraminifera and stable isotopes in Stjernsund show a constant influence of the NAC during the Early to Mid-Holocene period (9.3–5.0 ka BP), with temperatures similar to today's. A strong influence of AW is in line with the benthic foraminifer and stable isotope signal on the adjacent shelf, which support stable conditions.
- The absence of an HCO is explained by the strong influence of the NAC during the Early and Mid-Holocene.
- The faunal turnover and increased changes in the benthic isotope record during the Mid-Holocene Transition are probably related to the local sea-level fall and a general weakening of the NAC, which resulted in the enhanced influence of heat transfer processes between ocean and atmosphere.
- A gradual cooling of the bottom water of ~4°C across the late Holocene (2.5–0.2 ka BP) reflects an atmospheric signal induced by cold Arctic polar air masses. The cooling of the bottom water in Stjernsund might have been amplified by reduced NAC export strength.
- It is concluded that the atmospheric influence increased in the mid- and late Holocene owing to decreased connectivity of the fjord to the open shelf, which resulted from the local relative sea-level fall.
- In comparison with the adjacent shelf, the Stjernsund record shows additional short-term cooling events, which are suggested to be primarily atmospherically driven. At ~8.3, ~7.9, ~6.5, ~4.9, ~3.9 and ~3.3 ka BP, cold events in the bottom water are indicated by the $\delta^{18}O$ record. Except for the ~8.3 ka BP event, colder bottom-water temperatures are supported by the increased abundance of Arctic-Polar species. These cooling events are concurrent with fluctuations of the AW along the Norwegian shelf and with colder temperatures on land. Therefore it is concluded that short-term cold events may be induced through AW advection or through colder air temperatures induced by Arctic polar air masses. The relation of cold events to oceanic and atmospheric circulation variability is in line with climate reconstructions based on pollen and with recent observations of heat transfer processes between ocean and atmosphere.
- This study provides new insights to the regional climate development in northern Norway, which

was characterized by the interplay between the inflow of AW from the south and atmospherically induced temperature changes. The Stjernsund record showed that local heat transfer processes, such as the downward propagation of the air temperature signal, is a key mechanism to reflect climatic changes in bottom-water records of fjords.

Acknowledgements. – This study was part of the ESF-CARBONATE project funded by the Deutsche Forschungsgemeinschaft (DFG Fr-1134/16-1), with further funding within the EU-FP VII HERMIONE project (Contract number 226354). The captain and crew of RV 'Poseidon' are warmly thanked for their skilful support during the P325 cruise. The authors express their sincere thanks to S. Dorst, Kiel, who provided help with taxonomic questions. We would like to thank our student workers M. Streifert and S. Marali for sample preparation. They were funded through a generous grant to N. J. provided by the 'Präsidialfonds' of the University of Erlangen. The stable isotope measurements were skilfully carried out by M. Joachimski and D. Lutz at GeoZentrum Nordbayern. Isotopic analyses were funded through a Schmauser-Foundation grant to M.L.C. Radiocarbon dating was performed by T. Goslar at the Poznan Radiocarbon Laboratory, Poznan, Poland. We thank L. Hoffmann and M. Taviani for taxonomic identification of the molluscs, and P. Wintersteller for his support in producing the GIS maps. We greatly appreciate the constructive comments of A. Pieńkowski and an anonymous reviewer.

References

Andersen, C., Koç, N., Jennings, A. & Andrews, J. T. 2004a: Nonuniform response of the major surface currents in the Nordic Seas to insolation forcing: implications for the Holocene climate variability. *Paleoceanography 19*, PA2003, doi: 10.1029/2002PA000873.

Andersen, C., Koç, N. & Moros, M. 2004b: A highly unstable Holocene climate in the subpolar North Atlantic: evidence from diatoms: Holocene climate variability – a marine perspective. *Quaternary Science Reviews 23*, 2155–2166.

Andersson, C., Pausata, F. S. R., Jansen, E., Risebrobakken, B. & Telford, R. J. 2010: Holocene trends in the foraminifer record from the Norwegian Sea and the North Atlantic Ocean. *Climate of the Past 6*, 179–193.

Austin, W. & Scourse, J. D. 1997: Evolution of seasonal stratification in the Celtic Sea during the Holocene. *Journal of the Geological Society, London 154*, 249–256.

Belanger, P. E. & Streeter, S. S. 1980: Distribution and ecology of benthic foraminifera in the Norwegian–Greenland Sea. *Marine Micropaleontology 5*, 401–428.

Berger, A. 1978: Long-term variations of caloric insolation resulting from the earth's orbital elements. *Quaternary Research 9*, 139–167.

Berger, A. & Loutre, M. F. 1991: Insolation values for the climate of the last 10 million years. *Quaternary Science Reviews 10*, 297–317.

Bickert, T. 2006: Influence of geochemical processes on stable isotope distribution in marine sediments. *In* Schulz, H. D. & Zabel, M. (eds.): *Marine Geochemistry*, 339–369. Springer Verlag, Berlin.

Bjune, A. E., Birks, H. J. B. & Seppä, H. 2004: Holocene vegetation and climate history on a continental-oceanic transect in northern Fennoscandia based on pollen and plant macrofossils. *Boreas 33*, 211–223.

Bjune, A. E., Seppä, H. & Birks, H. J. B. 2009: Quantitative summer-temperature reconstructions for the last 2000 years based on pollen-stratigraphical data from northern Fennoscandia. *Journal of Paleolimnology 41*, 43–56.

Blindheim, J., Borovkov, V., Hansen, B., Malmberg, S. A., Turrell, W. R. & Østerhus, S. 2000: Upper layer cooling and freshening in the Norwegian Sea in relation to atmospheric forcing. *Deep Sea Research Part I: Oceanographic Research Papers 47*, 655–680.

Bond, G., Showers, W., Cheseby, M., Lotti, R., Almasi, P., de Menocal, P., Priore, P., Cullen, H., Hajdas, I. & Bonani, G. 1997: A pervasive millenial-scale cycle in North Atlantic Holocene and glacial climates. *Science 278*, 1257–1266.

Bondevik, S., Stormo, S. K. & Skjerdal, G. 2012: Green mosses date the Storegga tsunami to the chilliest decades of the 8.2 ka cold event. *Quaternary Science Reviews 45*, 1–6.

Calvo, E., Grimalt, J. & Jansen, E. 2002: High resolution U^{K}_{37} sea surface temperature reconstruction in the Norwegian Sea during the Holocene. *Quaternary Science Reviews 21*, 1385–1394.

Caralp, M. H. 1989: Abundance of *Bulimina exilis* and *Melonis barleeanum*: relationship to the quality of marine organic matter. *Geo-Marine Letters 9*, 37–43.

Chistyakova, N. O., Ivanova, E. V., Risebrobakken, B., Ovsepyan, E. A. & Ovsepyan, Y. S. 2010: Reconstruction of the postglacial environments in the southwestern Barents Sea based on foraminiferal assemblages. *Oceanology 50*, 573–581.

Conradsen, K. 1995: Late Younger Dryas to Holocene palaeoenvironments of the southern Kattegat, Scandinavia. *The Holocene 5*, 447–456.

Corliss, B. & Emerson, S. 1990: Distribution of Rose Bengal stained deep-sea benthic foraminifera from the Nova Scotian continental margin and Gulf of Maine. *Deep-Sea Research 37*, 381–400.

Corner, G. D., Nordahl, E., Munch-Ellingsen, K. & Robertsen, K. R. 1990: Morphology and sedimentology of an emergent fjord-head Gilbert-type delta: Alta delta, Norway. *Special Publications of the International Association of Sedimentologists 10*, 155–168.

Corner, G. D., Steinsund, P. I. & Aspeli, R. 1996: Distribution of recent benthic foraminifera in a subarctic fjord-delta: Tana, Norway. *Marine Geology 134*, 113–125.

Drange, H., Dokken, T., Furevik, T., Gerdes, R. & Berger, W. (eds.) 2005: The Nordic seas: an integrated perspective. *Geophysical Monograph 158*, 366 pp. American Geophysical Union, Washington DC.

Dullo, W.-C., Flögel, S. & Rüggeberg, A. 2008: Cold-water coral growth in relation to the hydrography of the Celtic and Nordic European continental margin. *Marine Ecology Progress Series 371*, 165–176.

Duplessy, J. C., Ivanova, E., Murdmaa, I., Paterne, M. & Labeyrie, L. 2001: Holocene paleoceanography of the northern Barents Sea and variations of the northward heat transport by the Atlantic Ocean. *Boreas 30*, 2–16.

Eilertsen, H. C. & Skarðhamar, J. 2006: Temperatures of north Norwegian fjords and coastal waters: variability, significance of local processes and air-sea heat exchange. *Estuarine, Coastal and Shelf Science 67*, 530–538.

Eiríksson, J., Bartels-Jónsdóttir, H. B., Cage, A. G., Gudmundsdóttir, E. R., Klitgaard-Kristensen, D., Marret, F., Rodrigues, T., Abrantes, F., Austin, W. E. N., Jiang, H., Knudsen, K.-L. & Sejrup, H.-P. 2006: Variability of the North Atlantic Current during the last 2000 years based on shelf bottom water and sea surface temperatures along an open ocean/shallow marine transect in western Europe. *The Holocene 16*, 1017–1029.

Emiliani, C. 1955: Pleistocene temperatures. *Journal of Geology 63*, 538–578.

Feyling-Hanssen, R. W. 1972: The foraminifer *Elphidium excavatum* (Terquem) and its variant forms. *Micropaleontology 18*, 337–354.

Filipsson, H. L. & Nordberg, K. 2010: Variations in organic carbon flux and stagnation periods during the last 2400 years in a Skagerrak fjord basin, inferred from benthic foraminiferal $\delta^{13}C$. *In* Howe, J. A., Austin, W. E. N., Forwick, M. & Paetzel, M. (eds.): *Fjord Systems and Archives*, 261–270. The Geological Society of London, London.

Freiwald, A., Dullo, W.-C. & Shipboard Party 2005: Unpublished cruise report. Leg 1: Bremerhaven-Tromsø, 12 July-24 July 2005; Leg 2: Tromø-Tromsø, 24 July-3 August 2005, p. 65.

Freiwald, A., Henrich, R. & Pätzold, J. 1997: Anatomy of a deep-water coral reef mound from Stjernsund, West Finnmark, Northern Norway. *Society of Economic Paleontologists and Mineralogists, Special Volume 56*, 141–162.

Furevik, T. 2001: Annual and interannual variability of Atlantic Water temperatures in the Norwegian and Barents Seas: 1980–

1996. *Deep Sea Research Part I: Oceanographic Research Papers 48*, 383–404.
Geslin, E., Heinz, P., Jorissen, F. & Hemleben, C. 2004: Migratory responses of deep-sea benthic foraminifera to variable oxygen conditions. *Marine Micropaleontology 53*, 227–243.
Giraudeau, J., Grelaud, M., Solignac, S., Andrews, J. T., Moros, M. & Jansen, E. 2010: Millennial-scale variability in Atlantic water advection to the Nordic Seas derived from Holocene coccolith concentration records. *Quaternary Science Reviews 29*, 1276–1287.
Gooday, A. 1993: Deep-sea benthic foraminiferal species which exploit phytodetritus: characteristic features and controls on distribution. *Marine Micropaleontology 22*, 187–205.
Gooday, A. & Lambshead, P. 1989: Influence of seasonally deposited phytodetritus on benthic foraminiferal populations in the bathyal northeast Atlantic: the species response. *Marine Ecology Progress Series 58*, 53–67.
Hald, M. & Aspeli, R. 1997: Rapid climatic shifts of the northern Norwegian Sea during the last deglaciation and the Holocene. *Boreas 26*, 15–28.
Hald, M. & Korsun, S. 1997: Distribution of modern benthic foraminifera from fjords of Svalbard, European Arctic. *Journal of Foraminiferal Research 27*, 101–122.
Hald, M. & Steinsund, P. I. 1992: Distribution of surface sediment benthic foraminifera in the southwestern Barents Sea. *Journal of Foraminiferal Research 22*, 347–362.
Hald, M., Andersson, C., Ebbesen, H., Jansen, E., Klitgaard-Kristensen, D., Risebrobakken, B., Salomonsen, G. R., Sarnthein, M., Sejrup, H. P. & Telford, R. J. 2007: Variations in temperature and extent of Atlantic Water in the northern North Atlantic during the Holocene. *Quaternary Science Reviews 26*, 3423–3440.
Hald, M., Danielsen, T. K. & Lorentzen, S. 1989: Late Pleistocene-Holocene benthic foraminiferal distribution in the southwestern Barents Sea: paleoenvironmental implications. *Boreas 18*, 367–388.
Hald, M., Husum, K., Vorren, T. O., Grøsfjeld, K., Jensen, H. B. & Sharapova, A. 2003: Holocene climate in the subarctic fjord Malangen, northern Norway: a multi-proxy study. *Boreas 32*, 543–559.
Hammer, Ø. & Harper, D. A. T. 2008: *Paleontological Data Analysis*. 351 pp. Blackwell Publishing, Oxford.
Hass, H. C. 1996: Northern Europe climate variations during late Holocene: evidence from marine Skagerrak. *Palaeogeography, Palaeoclimatology, Palaeoecology 123*, 121–145.
Heinz, P., Kitazato, H., Schmiedl, G. & Hemleben, C. 2001: Response of deep-sea benthic foraminifera from the Mediterranean Sea to simulated phytoplankton pulses under laboratory conditions. *The Journal of Foraminiferal Research 31*, 210–227.
Hermelin, J. O. R. 1986: Pliocene benthic foraminifera from the Blake Plateau: faunal assemblages and paleocirculation. *Marine Micropaleontology 10*, 343–370.
Hopkins, T. S. 1991: The GIN Sea – a synthesis of its physical oceanography and literature review 1972–1985. *Earth-Science Reviews 30*, 175–318.
Hurrell, J. W., Kushnir, Y. & Visbeck, M. H. (eds.) 2003: The North Atlantic Oscillation: climatic significance and environmental impact. *Geophysical Monograph 134*, 279 pp. American Geophysical Union, Washington DC.
Husum, K. & Hald, M. 2004a: Modern foraminiferal distribution in the subarctic Malangenfjord and adjoining shelf, Northern Norway. *Journal of Foraminiferal Research 34*, 34–48.
Husum, K. & Hald, M. 2004b: A continuous marine record 8000–1600 cal. yr BP from the Malangenfjord, north Norway: foraminiferal and isotopic evidence. *The Holocene 14*, 877–887.
Ingvaldsen, R. 2005: Width of the North Cape current and location of the Polar Front in the western Barents Sea. *Geophysical Research Letters 32*, L16603, doi: 10.1029/2005GL023440.
Jansen, E., Andersson, C., Moros, M., Nisancioglu, K. H., Nyland, B. F. & Telford, R. J. 2008: The early to mid-Holocene thermal optimum in the North Atlantic. *In* Battarabee, R. & Binney, H. (eds.): *Natural Climate Variability and Global Warming: A Holocene Perspective*, 123–137. Wiley-Blackwell, Oxford.
Jennings, A. E., Knudsen, K. L., Hald, M., Hansen, C. V. & Andrews, J. T. 2002: A mid-Holocene shift in Arctic sea-ice variability on the East Greenland Shelf. *The Holocene 12*, 49–58.
Johanessen, T. 1970: The climate of Scandinavia. *In* Wallén, C. (ed.): *Climates of Northern and Western Europe*, 23–79. Elsevier, Amsterdam.
Johnsen, S. J., Dahl-Jensen, D., Gundestrup, N., Steffensen, J. P., Clausen, H. B., Miller, H., Masson-Delmotte, V., Sveinbjörnsdottir, A. E. & White, J. 2001: Oxygen isotope and palaeotemperature records from six Greenland ice-core stations: Camp Century, Dye-3, GRIP, GISP2, Renland and NorthGRIP. *Journal of Quaternary Science 16*, 299–307.
Kaufman, D. S., Ager, T. A., Anderson, N. J. et al. 2004: Holocene thermal maximum in the western Arctic (0-180°W). *Quaternary Science Reviews 23*, 529–560.
Kaufman, D. S., Schneider, D., McKay, N., Ammann, C., Bradley, R., Briffa, K., Miller, G. H., Otto-Bliesner, B. L., Overpeck, J. T., Vinther, B. M. & Arctic lakes 2k Project Members 2009: Recent warming reverses long-term Arctic cooling. *Science 325*, 1236–1239.
Kjennbakken, H., Sejrup, H. P. & Haflidason, H. 2011: Mid- to late-Holocene oxygen isotopes from Voldafjorden, western Norway. *The Holocene 21*, 897–909.
Klitgaard-Kristensen, D., Sejrup, H. P. & Haflidason, H. 2001: The last 18 kyr fluctuations in Norwegian sea surface conditions and implications for the magnitude of climatic change: evidence from the North Sea. *Paleoceanography 16*, 455–467.
Klitgaard-Kristensen, D., Sejrup, H. F. & Haflidason, H. 2002: Distribution of recent calcareous benthic foraminifera in the northern North Sea and relation to the environment. *Polar Research 21*, 275–282.
Koç, N., Jansen, E. & Haflidason, H. 1993: Paleoceanographic reconstructions of surface ocean conditions in the Greenland, Iceland and Norwegian seas through the last 14 ka based on diatoms. *Quaternary Science Reviews 12*, 115–140.
Koç, N., Jansen, E., Hald, M. & Labeyrie, L. 1996: Late glacial-Holocene sea surface temperatures and gradients between the North Atlantic and the Norwegian Sea: implications for the Nordic heat pump. *In* Andrews, J. T., Austin, W. E. N., Bergsten, H. & Jennings, A. E. (eds.): *Late Quaternary Palaeoceanography of the North Atlantic Margin*, 177–185. The Geological Society of London, London.
Korsun, S. & Hald, M. 1998: Modern benthic foraminifera off Novaya Zemlya tidewater glaciers, Russian Arctic. *Arctic and Alpine Research 30*, 61–77.
Kucera, M. 2007: Planktonic foraminifera as tracers of past oceanic environments. *In* Hillaire-Marcel, C. & Vernal, A. (eds.): *Proxies in Late Cenozoic Paleoceanography*, 213–254. Elsevier, Amsterdam.
Lauritzen, S.-E. & Lundberg, J. 1999: Calibration of the speleothem delta function: an absolute temperature record for the Holocene in northern Norway. *The Holocene 9*, 659–669.
Lohmann, G. P. 1978: Abyssal benthonic foraminifera as hydrographic indicators in the western South Atlantic Ocean. *The Journal of Foraminiferal Research 8*, 6–34.
López Correa, M., Montagna, P., Joseph, N., Rüggeberg, A., Fietzke, J., Flögel, S., Dorschel, B., Goldstein, S., Wheeler, A. & Freiwald, A. 2012: Preboreal onset of cold-water coral growth beyond the Arctic Circle revealed by coupled radiocarbon and U-series dating and neodymium isotopes. *Quaternary Science Reviews 34*, 24–43.
Lubinski, D. J., Polyak, L. & Forman, S. L. 2001: Freshwater and Atlantic water inflows to the deep northern Barents and Kara seas since ca 13 ^{14}C ka: foraminifera and stable isotopes. *Quaternary Science Reviews 20*, 1851–1879.
Lutze, G. F. 1965: Zur Foraminiferen-Fauna der Ostsee. *Meyniana 15*, 75–142.
Lutze, G. F. 1974: Foraminiferen der Kieler Bucht (Westliche Ostsee): 1. 'Hausgartengebiet' des Sonderforschungsbereiches 95 der Universität Kiel. *Meyniana 26*, 9–22.
Mackensen, A. & Hald, M. 1988: *Cassidulina teretis* Tappan and *C. laevigata* d'Orbigny; their modern and late Quaternary distribution in northern seas. *Journal of Foraminiferal Research 18*, 16–24.

Mackensen, A., Fütterer, D. K., Grobe, H. & Schmiedl, G. 1993: Benthic foraminiferal assemblages from the eastern South Atlantic Polar Front region between 35° and 57°S: distribution, ecology and fossilization potential. *Marine Micropaleontology 22*, 33–69.

Mackensen, A., Sejrup, H. P. & Jansen, E. 1985: The distribution of living benthic foraminifera on the continental slope and rise off southwest Norway. *Marine Micropaleontology 9*, 275–306.

Maslin, M. A. & Swann, G. E. A. 2006: Isotopes in marine sediments. *In* Leng, M. J. (ed.): *Isotopes in Palaeoenvironmental Research*, 227–302. Springer, Dordrecht.

Mayewski, P. A., Rohling, E. E., Curt Stager, J., Karlén, W., Maasch, K. A., Meeker, D. L., Meyerson, E. A., Gasse, F., van Kreveld, S., Holmgren, K., Lee-Thorp, J., Rosqvist, G., Rack, F., Staubwasser, M., Schneider, R. R. & Steig, E. J. 2004: Holocene climate variability. *Quaternary Research 62*, 243–255.

McCrea, J. 1950: On the isotopic chemistry of carbonates and a paleotemperature scale. *Journal of Chemical Physics 18*, 849–857.

Mikalsen, G., Sejrup, H. P. & Aarseth, I. 2001: Late-Holocene changes in ocean circulation and climate: foraminiferal and isotopic evidence from Sulafjord, western Norway. *The Holocene 11*, 437–446.

Mork, M. 1981: Circulation phenomena and frontal dynamics of the Norwegian Coastal Current. *Philosophical Transactions of the Royal Society of London A302*, 635–647.

Murray, J. 2006: *Ecology and Applications of Benthic Foraminifera*. 426 pp. Cambridge University Press, Cambridge.

Nesje, A., Jansen, E., Birks, H., Bjune, A., Bakke, J., Andersson, C., Dahl, S., Klitgaard-Kristensen, D., Lauritzen, S.-E., Lie, Ø., Risebrobakken, B. & Svendsen, J.-I. 2005: Holocene climate variability in the northern North Atlantic region: a review of terrestrial and marine evidence. *In* Drange, H., Dokken, T., Furevik, T., Gerdes, R. & Berger, W. (eds.): *The Nordic Seas: An Integrated Perspective*, 289–322. American Geophysical Union, Washington, DC.

Nikulina, A., Polovodova, I. & Schönfeld, J. 2008: Foraminiferal response to environmental changes in Kiel Fjord, SW Baltic Sea. *eEarth Discussions 3*, 37–49.

Nomaki, H., Heinz, P., Nakatsuka, T., Shimanaga, M., Ohkouchi, N., Ogawa, N. O., Kogure, K., Ikemoto, E. & Kitazato, H. 2006: Different ingestion patterns of ^{13}C-labeled bacteria and algae by deep-sea benthic foraminifera. *Marine Ecology Progress Series 310*, 95–108.

Overland, J. E., Spillane, M. C., Percival, D. B., Wang, M. & Mofjeld, H. O. 2004: Seasonal and regional variation of pan-arctic surface air temperature over the instrumental record. *Journal of Climate 17*, 3263–3282.

Polyak, L. & Mikhailov, V. 1996: Post-glacial environments of the southeastern Barents Sea: foraminiferal evidence. *In* Andrews, J. T., Austin, W. E. N., Bergsten, H. & Jennings, A. E. (eds.): *Late Quaternary Palaeoceanography of the North Atlantic Margin*, 323–337. The Geological Society of London, London.

Poole, D. A. R. 1994: *Neogene and quaternary paleoenvironments on the north Norwegian Shelf*. Ph.D. thesis, University of Tromsø, 82 pp.

Rasmussen, T. L., Thomsen, E., Slubowska, M. A., Jessen, S., Solheim, A. & Koç, N. 2007: Paleoceanographic evolution of the SW Svalbard margin (76°N) since 20,000 ^{14}C yr BP. *Quaternary Research 67*, 100–114.

Rea, B. R. & Evans, D. J. A. 2007: Quantifying climate and glacier mass balance in north Norway during the Younger Dryas. *Palaeogeography, Palaeoclimatology, Palaeoecology 246*, 307–330.

Reimer, P. J., Baillie, M. G., Bard, E., et al. 2009: IntCal09 and Marine09 radiocarbon age calibration curves, 0-50,000 years cal BP. *Radiocarbon 51*, 1111–1150.

Renssen, H., Seppä, H., Heiri, O., Roche, D. M., Goosse, H. & Fichefet, T. 2009: The spatial and temporal complexity of the Holocene thermal maximum. *Nature Geoscience 2*, 411–414.

Risebrobakken, B., Dokken, T., Smedsrud, L. H., Andersson, C., Jansen, E., Moros, M. & Ivanova, E. V. 2011: Early Holocene temperature variability in the Nordic Seas: the role of oceanic heat advection versus changes in orbital forcing. *Paleoceanography 26*, PA4206, doi: 10.1029/2011PA002117.

Risebrobakken, B., Moros, M., Ivanova, E. V., Chistyakova, N. & Rosenberg, R. 2010: Climate and oceanographic variability in the SW Barents Sea during the Holocene. *The Holocene 20*, 609–621.

Rohling, E. & Cooke, S. 1999: Stable oxygen and carbon isotopes in foraminiferal carbonate shells. *In* Gupta, B. (ed.): *Modern Foraminifera*, 239–258. Kluwer Academic Publishers, Dordrecht.

Rohling, E. J. & Pälike, H. 2005: Centennial-scale climate cooling with a sudden cold event around 8,200 years ago. *Nature 434*, 975–979.

Romundset, A. & Bondevik, S. 2011: Propagation of the Storegga tsunami into ice-free lakes along the southern shores of the Barents Sea. *Journal of Quaternary Science 26*, 457–462.

Romundset, A., Bondevik, S. & Bennike, O. 2011: Postglacial uplift and relative sea level changes in Finnmark, northern Norway. *Quaternary Science Reviews 30*, 2398–2421.

Rüggeberg, A., Flögel, S., Dullo, W.-C., Hissmann, K. & Freiwald, A. 2011: Water mass characteristics and sill dynamics in a subpolar cold-water coral reef setting at Stjernsund, northern Norway: Special Issue on COld-water CArbonate Reservoir systems in Deep Environments – COCARDE. *Marine Geology 282*, 5–12.

Rytter, F., Knudsen, K. L., Seidenkrantz, M.-S. & Eiríksson, J. 2002: Modern distribution of benthic foraminifera on the north Icelandic shelf and slope. *Journal of Foraminiferal Research 32*, 217–244.

Schmiedl, G. 1995: Rekonstruktion der spätquartären Tiefenwasserzirkulation und Produktivität im östlichen Südatlantik anhand von benthischen Foraminiferenvergesellschaftungen. *Berichte zur Polarforschung 160*, 207 pp. Alfred-Wegener-Institut für Polar- und Meeresforschung, Bremerhaven.

Schmiedl, G. & Mackensen, A. 2006: Multispecies stable isotopes of benthic foraminifers reveal past changes of organic matter decomposition and deepwater oxygenation in the Arabian Sea. *Paleoceanography 21*, PA4213, doi: 10.1029/2006PA001284.

Schönfeld, J. 2001: Benthic foraminifera and pore-water oxygen profiles: a re-assessment of species boundary conditions at the western Iberian margin. *Journal of Foraminiferal Research 31*, 86–107.

Schönfeld, J. 2012: History and development of methods in Recent benthic foraminiferal studies. *Journal of Micropalaeontology 31*, 53–72.

Schröder, C. J., Scott, D. B. & Medioli, F. S. 1987: Can smaller benthic foraminifera be ignored in paleoenvironmental analyses? *Journal of Foraminiferal Research 17*, 101–105.

Schulz, H. D. & Zabel, M. (eds.) 2006: *Marine Geochemistry*. 574 pp. Springer Verlag, Berlin.

Sejrup, H. P., Birks, H. J. B., Klitgaard Kristensen, D. & Madsen, H. 2004: Benthonic foraminiferal distributions and quantitative transfer functions for the northwest European continental margin. *Marine Micropaleontology 53*, 197–226.

Sejrup, H.-P., Fjaeran, T., Hald, M., Beck, L., Hagen, J., Miljeteig, I., Morvik, I. & Norvik, O. 1981: Benthonic foraminifera in surface samples from the Norwegian continental margin between 62 degrees N and 65 degrees N. *Journal of Foraminiferal Research 11*, 277–295.

Sejrup, H. P., Haflidason, H., Flatebø, T., Kristensen, K., Grøsfjeld, K. & Larsen, E. 2001: Late-glacial to Holocene environmental changes and climate variability: evidence from Voldafjorden, western Norway. *Journal of Quaternary Science 16*, 181–198.

Seppä, H. & Birks, H. J. 2001: July mean temperature and annual precipitation trends during the Holocene in the Fennoscandian tree-line area: pollen-based climate reconstructions. *The Holocene 11*, 527–539.

Seppä, H. & Birks, H. J. B. 2002: Holocene climate reconstructions from the Fennoscandian Tree-Line area based on pollen data from Toskaljavri. *Quaternary Research 57*, 191–199.

Seppä, H., Bjune, A. E., Telford, R. J., Birks, H. J. B. & Veski, S. 2009: Last nine-thousand years of temperature variability in Northern Europe. *Climate of the Past 5*, 523–535.

Shackleton, N. J. 1974: Attainment of isotopic equilibrium between ocean water and the benthonic Foraminifera genus Uvigerina:

isotopic changes in the ocean during the last glacial. *Chargé de Recherches (CNRS), Colloques Internationales 219*, 203–209.
Shackleton, N. J. & Opdyke, N. D. 1973: Oxygen isotope and palaeomagnetic stratigraphy of Equatorial Pacific core V28-238: oxygen isotope temperatures and ice volumes on a 105 year and 106 year scale. *Quaternary Research 3*, 39–55.
Shemesh, A., Rosqvist, G., Rietti-Shati, M., Rubensdotter, L., Bigler, C., Yam, R. & Karlén, W. 2001: Holocene climatic change in Swedish Lapland inferred from an oxygen-isotope record of lacustrine biogenic silica. *The Holocene 11*, 447–454.
Skarðhamar, J. & Svendsen, H. 2005: Circulation and shelf-ocean interaction off North Norway. *Continental Shelf Research 25*, 1541–1560.
Ślubowska-Woldengen, M., Koç, N., Rasmussen, T. L., Klitgaard-Kristensen, D., Hald, M. & Jennings, A. E. 2008: Time-slice reconstructions of ocean circulation changes on the continental shelf in the Nordic and Barents Seas during the last 16,000 cal yr B.P. *Quaternary Science Reviews 27*, 1476–1492.
Vinther, B. M., Buchardt, S. L., Clausen, H. B., Dahl-Jensen, D., Johnsen, S. J., Fisher, D. A., Koerner, R. M., Raynaud, D., Lipenkov, V., Andersen, K. K., Blunier, T., Rasmussen, S. O., Steffensen, J. P. & Svensson, A. M. 2009: Holocene thinning of the Greenland ice sheet. *Nature 461*, 385–388.
Wanner, H., Solomina, O., Grosjean, M., Ritz, S. P. & Jetel, M. 2011: Structure and origin of Holocene cold events. *Quaternary Science Reviews 30*, 3109–3123.
Wick, W. 1947: Aufbereitungsmethoden in der Mikropaläontologie. *Jahresberichte der Naturhistorischen Gesellschaft Hannover 98*, 35–41.
Wu, G. & Berger, W. H. 1989: Planktonic foraminifera: differential dissolution and the Quaternary stable isotope record in the west equatorial Pacific. *Paleoceanography 4*, 181–198.

Supporting information

Additional Supporting Information may be found in the online version of this article:

Table S1. Age interpolation, foraminiferal census data and stable isotope record of core POS-325-482. The abundances of benthic foraminifera are reported in percentage of the total benthic fauna, while the percentage of the planktonic foraminifera are referred to the total foraminiferal fauna.

Table S2. Benthic foraminiferal species found in Stjernsund core POS-325-482-2. Note: taxonomic references were given by Ellis and Messina (1940–2011). They are not included in the reference list. Indented species were identified using the indicated secondary literature.